M.Sc. Thesis
Master of Science in Sustainable Energy
Master of Science in Thermal Energy Engineering

DTU Management Engineering
Department of Management Engineering

Analysis of solar heating / heat pump systems

Carlos Jurado (s152084)

Kongens Lyngby 2020

DTU

DTU Management Engineering
Department of Management Engineering
Technical University of Denmark

DTU Civil Engineering
Department of Civil Engineering
Technical University of Denmark
Brovej, Building 118
Building 303B
2800 Kongens Lyngby, Denmark
Phone +45 25 17 00
www.byg.dtu.dk

Dedicated to my mom Emma,

The most important person in my life

No one can go back and start over,

but anyone can start today and make a new ending

Jared Leto

Preface

This thesis was prepared at the Department of Civil Engineering, Technical University of Denmark as requirement to fulfilment of the requirements for the Master of Science of Sustainable Energy - Thermal Energy.

The project was carried out from February to August 2020 under the supervision of Elsabet Nomonde Noma Nielsen and Simon Furbo (DTU Department of Civil Engineering). The project is credited with 30 ECTS points.

Carlos Jurado (s152084)

Acknowledgements

I am grateful to study in this prestigious University. It has been 2 years of a great experience where I have met wonderful people.

I want to thank my supervisors for all their help and invested time in the project, their patience throughout the project despite the current circumstances we are living.

Likewise all my friends and family who encouraged me to keep going.

Summary

Since one of the main goals of this decade is to reduce global warming and all the related impacts linked to this, the generation of energy through renewable energy sources (RES) is indispensable. Considering the need of production of domestic hot water (DHW) and space heating (SH) in the residential sector, the development of combined solar heating/heat pump systems can contribute to the generation of clean energy reducing impact on the environment.

"Solar heating/heat pump system with horizontal ground source heat exchanger" is one of the experimental investigations on solar heating/heat pump systems for single family houses at DTU. The test facility is located at Department of Civil Engineering and started in 2013. An analysis based on the data collected from the test facility at the Climate Station at DTU Byg. Weather conditions, volume flow rates measured in the different loops and temperatures in different measurement points of the system were used to study the solar radiation on the ground and investigate the influence of the ambient conditions on the ground. An analysis of temperatures on the Horizontal ground source heat exchanger was carried out in order to evaluated the heat transfer between the pipes and the soil. The power and the heat exchange capacity rate were calculated for different operational modes.

A model of the HGSHE was developed on Transient System Simulation Tool (TRNSYS) software, different parameters were calculated and the Kusuda correlation was used in order to calculate key parameters. An iteration of values was carried out in order to find the pipe soil contact resistant. This value set a outlet temperature of the fluid as close as possible to the measured outlet temperature. The results shows that both temperatures differ less than 1 K for monthly simulation.

Contents

Preface i

Acknowledgements ii

Summary iii

Contents iv

List of Figures v

List of Tables vii

Nomenclature viii

Contents x

1 Introduction 1
- 1.1 Background . . . 1
- 1.2 Details of the combined solar heating/heat pump system . . . 2

2 Analysis framework 12
- 2.1 Analysis of the solar radiation on the solar collector . . . 12
- 2.2 Analysis of the global radiation on the ground . . . 15
- 2.3 Analysis on the Horizontal ground source heat exchanger (HGSHE) . . . 19
- 2.4 Analysis of Temperatures on the HGSHE . . . 23
- 2.5 Analysis of the Heat exchange capacity rate (HECR) and Power . . . 29

3 Simulation on TRNSYS 33
- 3.1 HGSHE TRNSYS model . . . 33
- 3.2 Soil model on TRNSYS . . . 36
- 3.3 Start temperature profiles . . . 36
- 3.4 Pipe soil contact resistant (PSCR) and Simulations . . . 38

4 Results 43

5 Conclusion 45

A An Appendix 47

References 52

List of Figures

1.1 Combined solar heating/heat pump system with HGSHE . . . 2
1.2 Layout of the HGSHE . . . 3
1.3 Cross section A-A HGSHE [3] . . . 4
1.4 Pictures of storage tank-in-tank . . . 4
1.5 Kingspan solar collector . . . 5
1.6 Heat pump (heating capacity of 3-12 kW) . . . 6
1.7 DHW and SH heat sink sources . . . 7
1.8 Charging process storage tank heat pump in operation . . . 7
1.9 Charging process storage solar collector in operation . . . 8
1.10 Discharging process storage tank . . . 8
1.11 Measurement components solar heating/heat pump system [3] . . . 9

2.1 Energy flows in the system . . . 13
2.2 Energy balance January 2019 . . . 14
2.3 Energy balance July 2019 . . . 14
2.4 HGSHE diagram and temperature sensors location . . . 15
2.5 Ground temperatures analysis July 2019 . . . 16
2.6 Ground temperatures analysis February 2019 . . . 16
2.7 Ground temperatures analysis 5 to 10 July . . . 17
2.8 Ground temperatures analysis 18 to 21 October . . . 17
2.9 Monthly temperature at noon in different depths January 2019 . . . 18
2.10 Monthly temperature at noon in different depths July 2019 . . . 18
2.11 Diagram of the pipes system of the HGSHE . . . 19
2.12 Slings in HGSHE . . . 20
2.13 Selection of time ahead for ground temperatures for sling 1 . . . 21
2.14 Temperatures HGSHE t=0 min, pump P3 in operation July 9 . . . 23
2.15 Temperatures close to the pipes t=23 min July 9 . . . 24
2.16 Temperatures HGSHE t=23 min, pump P3 in operation July 9 . . . 25
2.17 Temperatures analysis 9 July . . . 25
2.18 Temperatures analysis 22 August 2019 . . . 26
2.19 Ground temperature analysis, June 12 (rainy period) . . . 26
2.20 Temperatures HGSHE t=0 min, Heat pump in operation January 27 . . . 27
2.21 Temperatures HGSHE t=13 min, Heat pump in operation January 27 . . . 28
2.22 Ground temperatures close to the pipes, January 27 . . . 28
2.23 Nodes diagram HGSHE . . . 30
2.24 Power and HECR, July 9 . . . 30
2.25 Power and HECR, January 27 . . . 31
2.26 Analysis Tground, Power and HECR, SC in operation . . . 31
2.27 Analysis Tground, Power and HECR, HP in operation . . . 32

3.1 2D boundary conditions HGSHE model . . . 33
3.2 HGSHE TRNSYS model . . . 34
3.3 Connection between pipe and flow diverter . . . 35

3.4 Inputs and Outputs TRNSYS model 35
3.5 Measured temperature profiles 1st day of the month 2019 at noon 36
3.6 Calculated and measured temperature profile July 1 at noon 37
3.7 Iteration method PSCR January 1 38
3.8 Analysis (T13 M-T13 C) with different PSCR (T14 < -0.5 °C) January 2019 gr- HP 39
3.9 Analysis (T13 M-T13 C) with different PSCR (6.38 °C <T14 < 10°C) January 2019 (SC-gr) 39
3.10 ΔT differences (T13 M-T13 C) for T14 intervals January 40
3.11 Analysis (T13 M-T13 C) with different PSCR (T14 > 30°C) July SC-gr 40
3.12 ΔT differences (T13 M-T13 C) for T14 intervals July 41
3.13 Monthly PSCR values for both operational modes 41
3.14 TRNSYS simulation January 3 42
3.15 TRNSYS simulation July 23 42

4.1 Energy quantities 2019 44
4.2 Seasonal Performance Factors (SPF) 44

A.1 Energy balance February 2019 47
A.2 Energy balance March 2019 48
A.3 Energy balance May 2019 48
A.4 Energy balance June 2019 49
A.5 Energy balance August 2019 49
A.6 Energy balance September 2019 50
A.7 Energy balance October 2019 50
A.8 Energy balance November 2019 51
A.9 Energy balance December 2019 51

List of Tables

1.1 Position of temperature sensors in storage tank 10
1.2 Position of pipes in the storage tank 10
1.3 Measurement equipment of solar collector loop 10

2.1 Complete cycle time, pump P3 in operation 20
2.2 System cycle time node by node, pump P3 in operation 21
2.3 Complete cycle time, heat pump in operation 22
2.4 System cycle time node by node, heat pump in operation 22

3.1 Monthly T_{amp} 38

Nomenclature

Abbreviations

DTU	Technical University of Denmark	RES	Renewable energy sources
DHW	Domestic hot water	SH	Space heating
$HGSHE$	Horizontal ground source heat exchanger	GMT	Greenwich Mean Time
$TRNSYS$	Transient System Simulation Tool	HP	Heat pump
SC	Solar collector	$PE80$	Polyethylene pipe type 80
IPA	Isopropyl alcohol	B	Borehole
H	Hose	PP	Polypropylene
POM	Polyoxymethylene	PEX	Polyethylene
M	Motor valve	P	Pump
R	Thermostatic valve	DCW	Domestic cold water
TSR	Total solar radiation	$HECR$	Heat exchange capacity rate
R	Thermostatic valve	DCW	Domestic cold water
Jan	January	Feb	February
Mar	March	Apr	April
May	May	Jun	June
Jul	July	Aug	August
Sep	September	Oct	October
Nov	November	Dec	December
FD	Flow diverter	FF	Far field
z	depth	FF	Far field
fig	figure	Eq	Equation
$diff$	difference		

Greek letters

Δ	Difference [K]	ρ	Density $[\frac{kg}{m^3}]$
$\sum$	sum	α	Thermal diffusivity $[\frac{m^2}{s}]$

Symbols

$Power$	Power $[kW]$	V	volume $[m^3]$
SPF	Seasonal performance factor $[-]$	COP	Coefficient of performance $[-]$
E	Energy $[kWh]$	T	Temperature [°C]
Qf	Fluid flow $[\frac{m^3}{min}]$	t	Time $[min]$
TH	Ground temperature close to pipe $[°C]$	Tg	Average ground temperature sling $[°C]$
$\dot{V}$	Volume flow $[\frac{l}{min}]$	Cp	Heat capacity $[\frac{J}{K}]$
$LMTD$	Logarithmic mean temperature difference [°C]	Q	Thermal energy $[kWh]$
$PSCR$	Pipe soil contact resistance $[\frac{m^2*K}{W}]$	k	Thermal conductivity of the soil layer
exp	exponential function [-]	k	Thermal conductivity of the soil layer
μ	viscosity $[\frac{kg}{m*s}]$	k	Thermal conductivity of the soil layer

Superscripts

p	pump	m	mean
gr	ground	HP	heat pump
cts	control system	mv	motorized valves
cp	circulation pump	$solar$	solar
tot	total	ave	min
minimum			
M	measured	C	Calculated

Subscripts

z	depth	day	day

Contents

Preface i

Acknowledgements ii

Summary iii

Contents iv

List of Figures v

List of Tables vii

Nomenclature viii

Contents x

1 Introduction 1
- 1.1 Background . . . 1
- 1.2 Details of the combined solar heating/heat pump system . . . 2

2 Analysis framework 12
- 2.1 Analysis of the solar radiation on the solar collector . . . 12
- 2.2 Analysis of the global radiation on the ground . . . 15
- 2.3 Analysis on the Horizontal ground source heat exchanger (HGSHE) . . . 19
- 2.4 Analysis of Temperatures on the HGSHE . . . 23
- 2.5 Analysis of the Heat exchange capacity rate (HECR) and Power . . . 29

3 Simulation on TRNSYS 33
- 3.1 HGSHE TRNSYS model . . . 33
- 3.2 Soil model on TRNSYS . . . 36
- 3.3 Start temperature profiles . . . 36
- 3.4 Pipe soil contact resistant (PSCR) and Simulations . . . 38

4 Results 43

5 Conclusion 45

A An Appendix 47

References 52

CHAPTER 1

Introduction

In this chapter is presented a general introduction of one of the ongoing projects carried out at Department of Civil Engineering, Technical University of Denmark (DTU). "Solar heating/heat pump system with horizontal ground source heat exchanger" is one of the experimental investigations on solar heating/heat pump systems for single family houses at DTU. The test facility is located at Department of Civil Engineering and started in 2013. The project is financed by the Bjarne Saxhof foundation.

The aim of the project is to increase the knowledge on the design of these kind of models and the understanding in a better way of the heat and mass transfer process in combined systems. Data collected in 2019 will be used to analyze different periods in order to determine the behavior of the ground temperatures and the different components of the system under certain conditions. The analysis is focused on the horizontal ground source heat exchanger (HGSHE), a model of the HGSHE will be develop on Transient System Simulation Tool (TRNSYS) software in order to determine the pipe soil contact resistant (PSCR) month by month. The PSCR indicates the resistance to heat transfer between the pipe and soil boundary, a lower value of PSCR means a higher heat transfer.

1.1 Background

Since one of the main goals of this decade is to reduce global warming and all the related impacts linked to this, the generation of energy through renewable energy sources (RES) is indispensable. Considering the need of production of domestic hot water (DHW) and space heating (SH) in the residential sector, the development of combined solar heating/heat pump systems can contribute to the generation of clean energy reducing impact on the environment.

The main aspect in terms of the operation in this kind of combined systems is the reduction of the heat pump energy consumption. Solar energy can be used to increase the inlet temperature in the heat pump; thus, the performance of the system will be higher. The main components of these systems are solar collectors, heat pumps, heat exchangers and storage tanks. The configuration of the system can be arranged according to the needs. Unfortunately, the experiences from the systems put in operation are often not as positive as expected. The efficiency of the systems is low, and the systems are relatively costly and complicated [3].

Previous studies have been carried out focused on different parameters of combined solar heating/heat pump systems, [5] focused on solar thermal regeneration of the soil analyzing both numerical modelling on TRNSYS and experimental investigations using heat pumps coupled with a horizontal ground source heat exchanger (HGSHE) and a solar collector. Different kind of soils were used during the investigation and the optimal size of HGSHE was calculated.

[7] developed a numerical model on TRNSYS using a dual source heat pump coupled with a HGSHE with 0.2 m of depth, a solar collector with a surface area equal to 8 m^2 using water

as fluid. The conclusions and results of the study show that the outlet temperature of the water in the level of heat exchanger increases by augmenting the depth. The coefficient of performance (COP) of the Heat pump is higher when the solar collector area is higher.

[2] presented a comparative study of heat transfer in seven ground media. It was investigated how excess electricity produced from solar PV panels can be more efficiently stored in an insulated HGSHE to heat a 15 m2 test room with a heating load of 1 kW during the typical winter conditions in Nottingham, UK. An experimental HGSHE was set-up using two soil types as backfill media including sand and gravel. It was evaluated the performance of the system in heating mode (charging) and extracting mode (discharging).Sand and GR gravel soils showed the best heat storage performance properties, retaining heat for longer periods and cooling slower compared to other tested sands.

1.2 Details of the combined solar heating/heat pump system

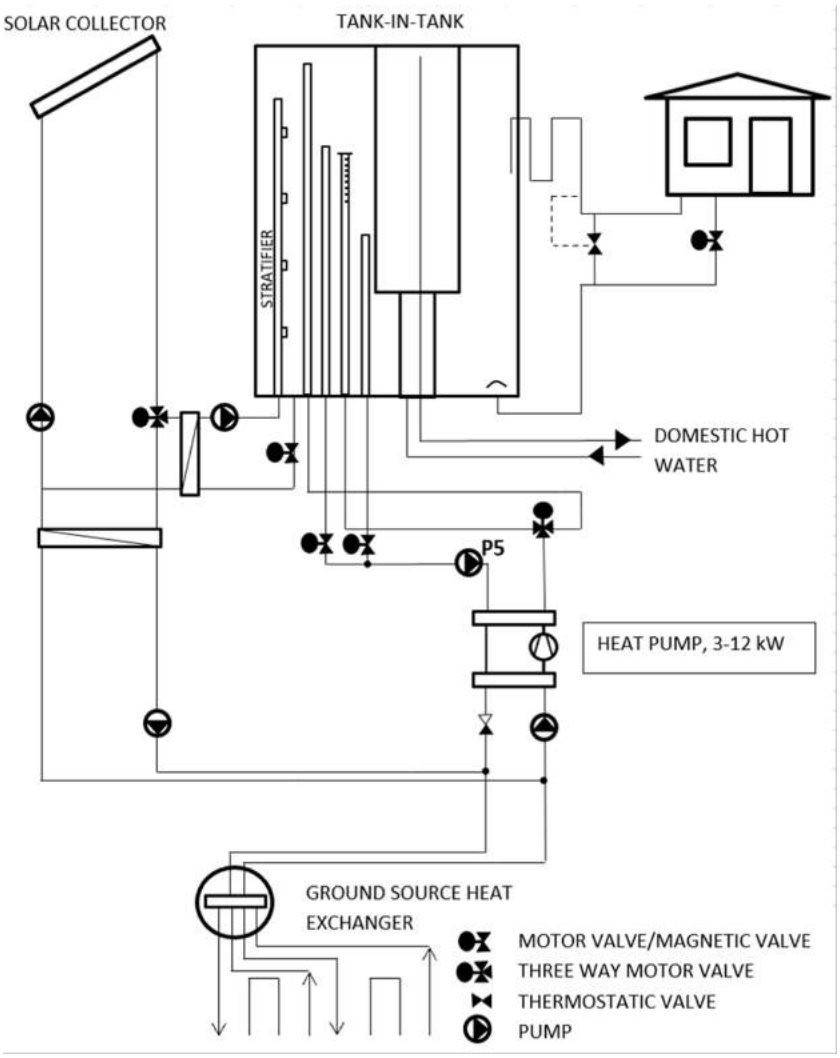

Figure 1.1: Combined solar heating/heat pump system with HGSHE.

The system consists of a storage tank-in-tank with volumes DHW and SH, a solar collector and a heat pump coupled with a HGSHE. DHW and SH are distributed to a distribution system from the storage tank to simulate the consumption of DHW and SH in a single family house. Figure 1.1 shows a scheme of the combined system [3]. Each of the components are described in detail below.

1.2.1 Horizontal ground source heat exchanger (HGSHE)

Figure 1.2 shows a sketch of the HGSHE, this covers an area of 30 x 8.5 m. The HGSHE laid 1 m below the soil surface and the polyethylene pipes are type PE80 with 40 and 35.4 mm of outside and inner diameter respectively, the separation between the pipes is 1.2 m. The length of each pipe is 30 m and the HGSHE is divided into 2 slings, each sling contains 4 pipes or hoses (total length of each sling 120 m). The flow is divided into the slings via a sump or manifold, feeding tubes are the connection between the HGSHE and the heat pump, the outside and inner diameter of these tubes are 40 and 35.4 mm respectively. The fluid used in the operation is a mixture of 50 % isopropyl alcohol (IPA) and 50 % water. Figure 1.2 also shows 2 boreholes drilled to a depth of 10 m, B1 which is located 10 m away from the edge of the HGSHE and B2 located beside the edge of the HGSHE in the opposite direction. The aim is to measure ground temperature in 2 different locations each meter until 10 m below the soil surface. Figure 1.3 shows the distribution of the sensors for borehole B2 [3].

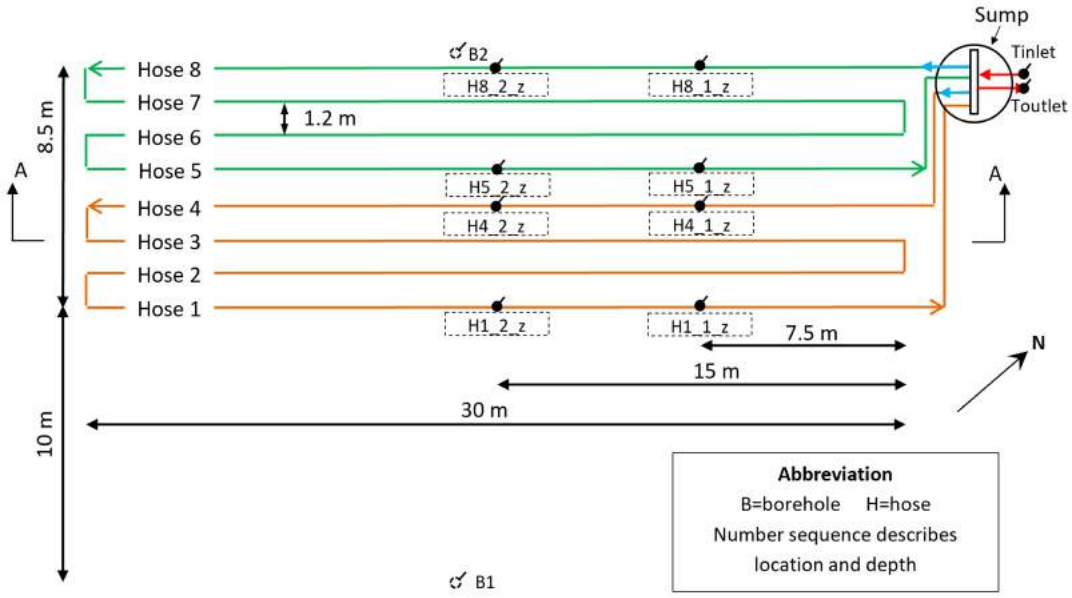

Figure 1.2: Layout of the HGSHE.

Furthermore, ground temperatures sensors are located close to the hoses 8, 5, 4 and 1. The aim is to measure the ground temperature close to the pipes and analyze the influence of the process on the soil. These sensors are located at different depths as it is shown in figure 1.3, 0.5 m, 1 m and 1.5 m below the soil surface. 2 groups of sensors are positioned per sling to analyze the distribution of the temperatures.

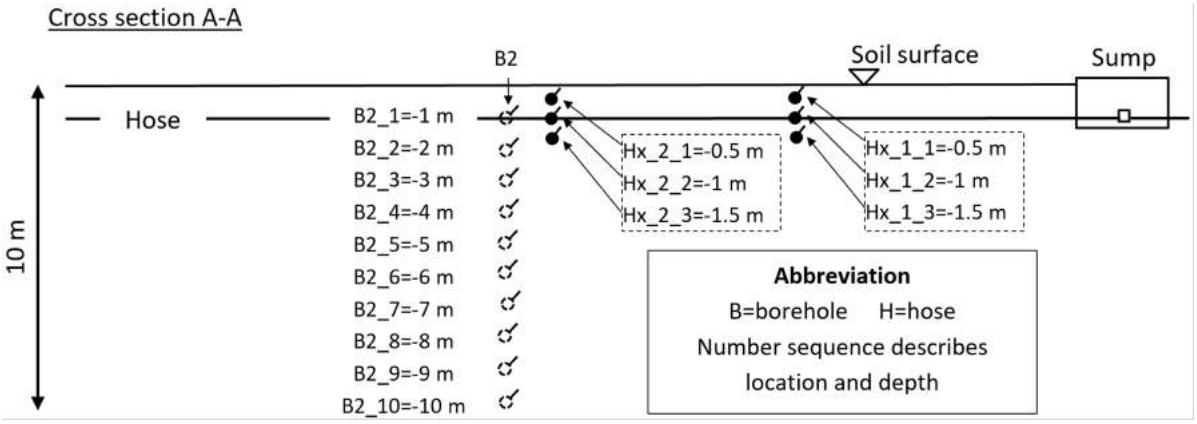

Figure 1.3: Cross section A-A HGSHE [3].

1.2.2 The storage tank

The storage is a tank-in-tank manufactured by the Danish company Ajva ApS. Figure 1.4 shows pictures of the tank-in-tank storage without and with insulation [3]. The capacity of the tank is 725 l distributed in 550 l for DHW and 175 l for space heating. In the outer tank, there is a stratification pipe made of polypropylene (PP) with an outer diameter of 60 mm and a wall thickness of 3 mm. The opening orifices act as check valves allowing the water flows only in one direction via this pipe, the energy from the solar collector will be transferred to the tank. Additionally to this, 4 more pipes are installed inside the tank which will be used to transfer energy from the heat pump, these are made of polyoxymethylene (POM) with an outer diameter of 80 mm and an inner diameter of 35 mm. Figure 1.2 shows the configuration of the pipes inside the tank-in-tank.

Figure 1.4: Pictures of storage tank-in-tank.

In terms of the 4 pipes which are used to provide energy from the heat pump, pipe 1 and 3 (from left to right) are used to charge the tank and the others are return pipes. Depending the operational mode, water will the transferred to the top of the tank if DHW is produced or to the middle of the tank if SH is produced. DHW is taken from the top of the tank and transferred to the distribution system via a crosslinked polyethylene (PEX) pipe. On the other

hand, SH is taken from the middle of the tank via a bended pipe (see fig. 1.2), This pipe is made of composite plastic and aluminum. The tank contain a half ball baffle plate with a diameter of 200 mm in the SH return pipe in order to avoid mixing in the storage.

1.2.3 The solar collector

The solar collectors (SC) are type evacuated tubular collectors with a surface area of 9.6 m^2 manufactured by the company Kingspan. The collector slope is 45°. The SC is facing south 12° toward east from south. Depending the operational mode, the energy is transferred to the tank or to the ground via plate heat exchangers using a 3 way motor valve (M7). The system operates using circulation pumps in the primary and secondary loop type NMT Plus 25-80180 from IMP PUMPS (P1) (see figure 1.11) and type UPS 25-40-180 from Grundfos (P2) (see figure 1.11) respectively. 2 flow meters are installed in the primary and secondary loop in order to measure the volume flow. Figure 1.5 shows a picture of a evacuated solar collector as reference.

Figure 1.5: Kingspan solar collector.

1.2.4 The heat pump

A heat pump manufactured by the Danish company Salling vaske- og køleservice A/S with a heating capacity of 3-12 kW is used as auxiliary energy source, the coolant is type R134a. Figure 1.6 shows pictures of the heat pump and its components [3]. There are 2 circulation pumps in this loop, the first used to transfer energy from the condenser of the heat pump to the storage tank (P5) (see figure 1.11) and a second pump between the HGSHE and the heat pump (P6) (see figure 1.11). The first one is type Alfa 1 25-60-180 from Grundfos and the other one is type Magna 25-60-180 from Grundfos. Additionally, the control system of the heat pump is based on inputs from different temperature sensors. These sensors can be seen in figure 1.11, they are located in specific locations in order to determine the operational mode of the system. The temperature sensors are type LMC 320 are type NTC with an accuracy of ±1 K.

In order to direct the flow according the priority of production of DWH or SH, a 3-way motor valve is used between the heat pump and the tank (M6) (see figure 1.11). The priority of the system is the production of DHW. In order to reach the set points of production of DHW or SH, the compressor of the heat pump operates on a nominal compressor frequency of 50 Hz in on/off mode, but, also, it can operate in a modulating mode using a frequency inverter which allows it to operate in a range between 30 Hz and 70 Hz, the electricity consumption

will be higher if the operation frequency is higher.

Figure 1.6: Heat pump (heating capacity of 3-12 kW).

The set points for the production of DHW is determined by the temperature sensor T3 (see figure 1.11). When T3 is below the set point, the pump starts to operate and stops when T3 is above the base line plus a established ΔT. On the other hand, when the production of SH is required, the set point is determined by T6 (see figure 1.11). The details of the different operational modes will be extended in the subsection of control strategy.

1.2.5 Domestic hot water (DHW) loop and space heating (SH) loop configurations

Figure 1.7 shows the pictures of the components which simulate the consumption of DHW and SH in the facility for a single family house [3]. A buffer tank (right) which is insulated act as heat sink source for the DHW production, meanwhile, a cooling system combined with a insulated tank (left) has the same function for the SH production. Additionally, these components contain motorized valves types Honeywell to activate the SH and DHW loops of the combined system. In terms of the SH production, a thermostatic valve from Danfoss (R1) is located between the distribution and the return line in order to mix cold and hot water if it is needed. At the moment, the valve is not activated.

In order to simulate the consumption of DHW and SH, it is needed to set parameters of consumption for each mode. In terms of DHW, 4.5 kWh of energy are tapped every day, DHW is drawn 3 times per day in equal amounts (morning, afternoon and evening), the volume flow rate during the tapping is around 7.5 l/min. In the case of SH consumption, water is drawn with a flow rate of 5 l/min. The demand of SH is related with the monthly space heating demand for a single family house of 140 m^2 with, a yearly space heating demands per m^2 floor area of 30 kWh (SFH 30) corresponding to a yearly space heating demand of about 4700 kWh [3]. No SH consumption is provided from May to September.

Figure 1.7: DHW and SH heat sink sources.

1.2.6 Operational modes of the combined system

In order to provide hot water to the storage tank or heat to the ground from the solar collector, it is needed to establish set points for the operation of the solar collector and the heat pump. In terms of the storage tank, the priority for both systems is the production of DHW, the second one is the production of SH. Figure 1.8 shows the different charging processes for the storage tank when the heat pump is in operation [3], production of DHW from the heat pump (left) and production of SH from the heat pump (right). Figure 1.9 shows the operational mode when the solar collector is in operation [3], energy is transferred to the tank using the stratifier pipe (left). If the needs of energy are satisfied in the storage tank, heat can be transferred from the solar collector to the ground (right). Both subsystems can operate at the same time.

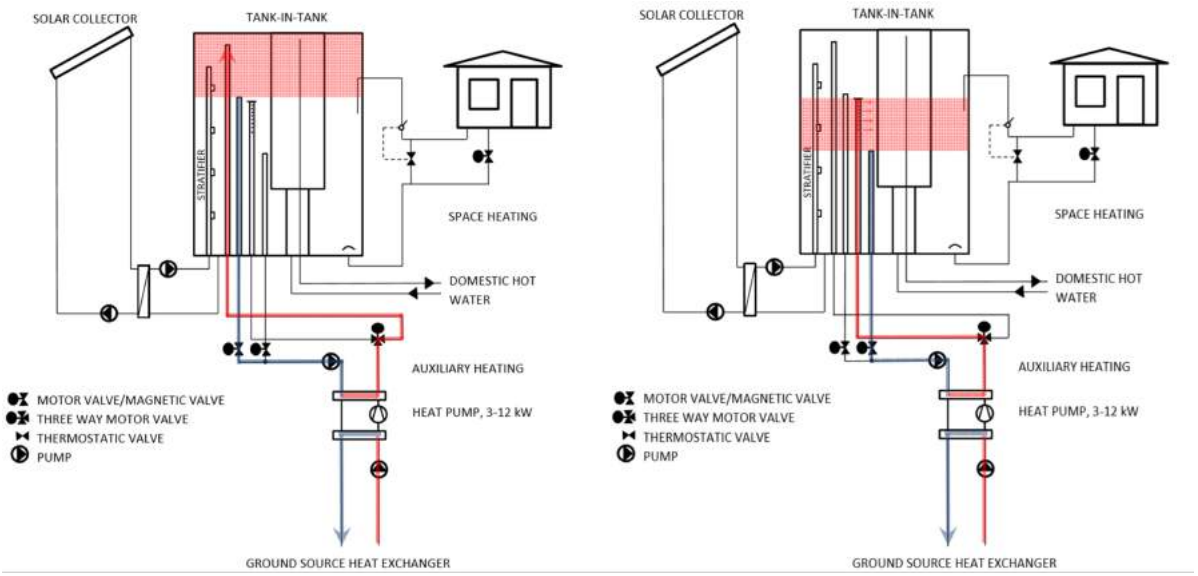

Figure 1.8: Charging process storage tank heat pump in operation.

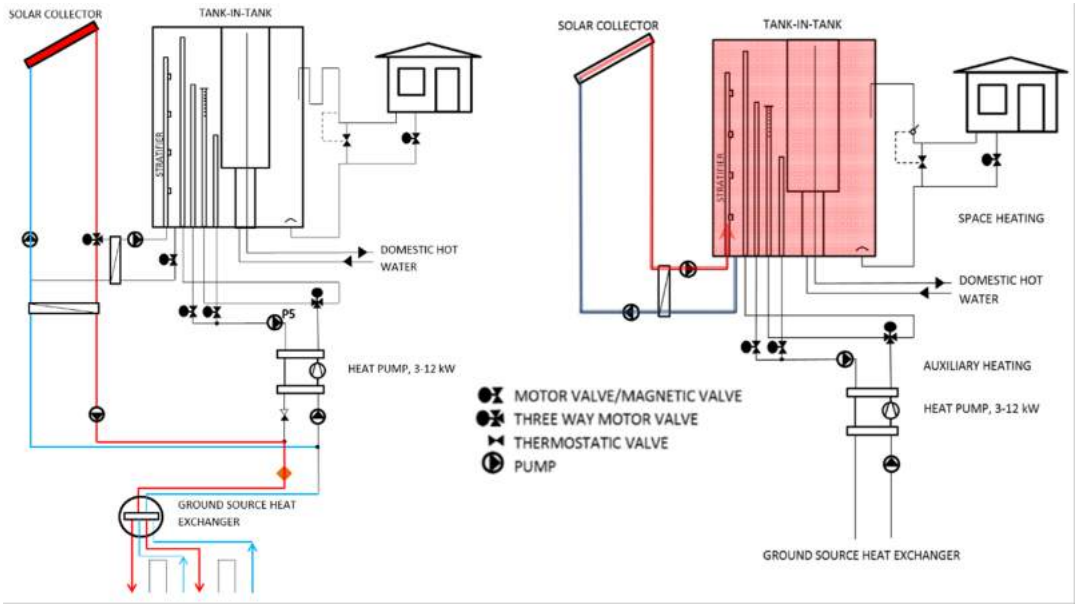

Figure 1.9: Charging process storage solar collector in operation.

Figure 1.10 shows the discharging process of DHW and SH in the facility [3]. DHW is taken from the top of the tank, the storage is filled with cold water to compensate the draw off. SH water is taken from the middle of the tank and returns to the tank via a pipe located on the bottom of the storage.

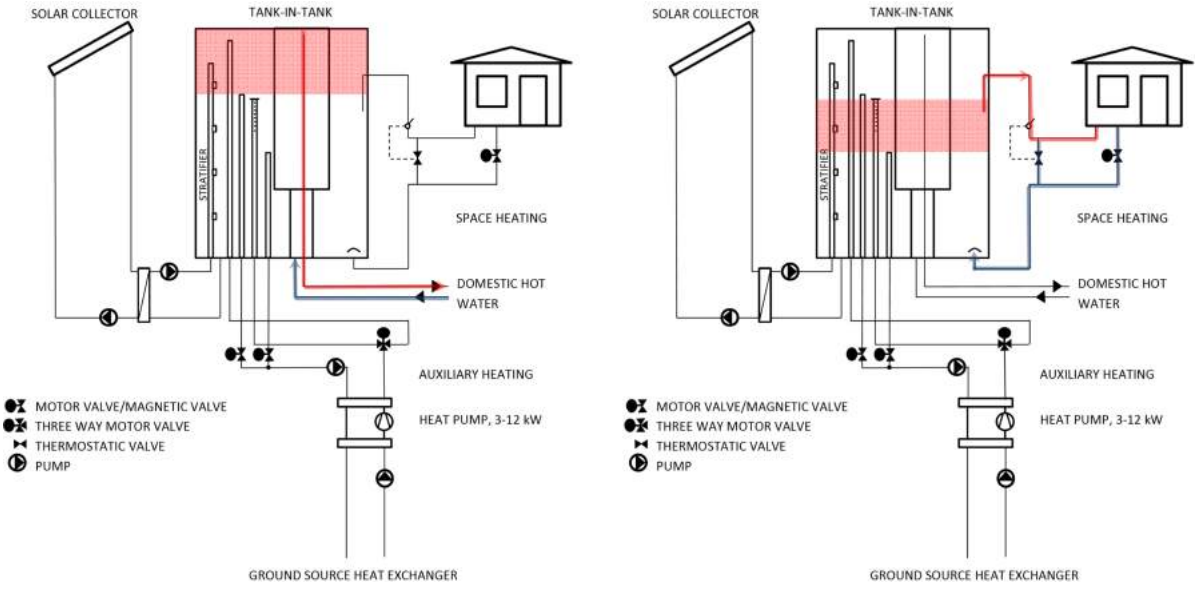

Figure 1.10: Discharging process storage tank.

1.2.7 Control strategy solar heating/heat pump system

These kind of systems need to set some parameters in order to establish the operational mode. Temperature sensors, flow meters and motorized valves are used for this purpose. Figure 1.11 shows the locations of the different measurement components, table 1.1 shows the location of the different temperature sensors used for control system and monitoring, table 1.2 shows the positions of pipes in the tank. Control system means that these measurement points are

used to determine the operational mode of the system. For example, if the solar collector will transfer energy to the tank or to the ground. In the case of the heat pump, if this will produce DHW or SH energy to the tank. On the other hand, the monitoring system means that these reference temperatures set the draw off for DHW or SH to the facility.

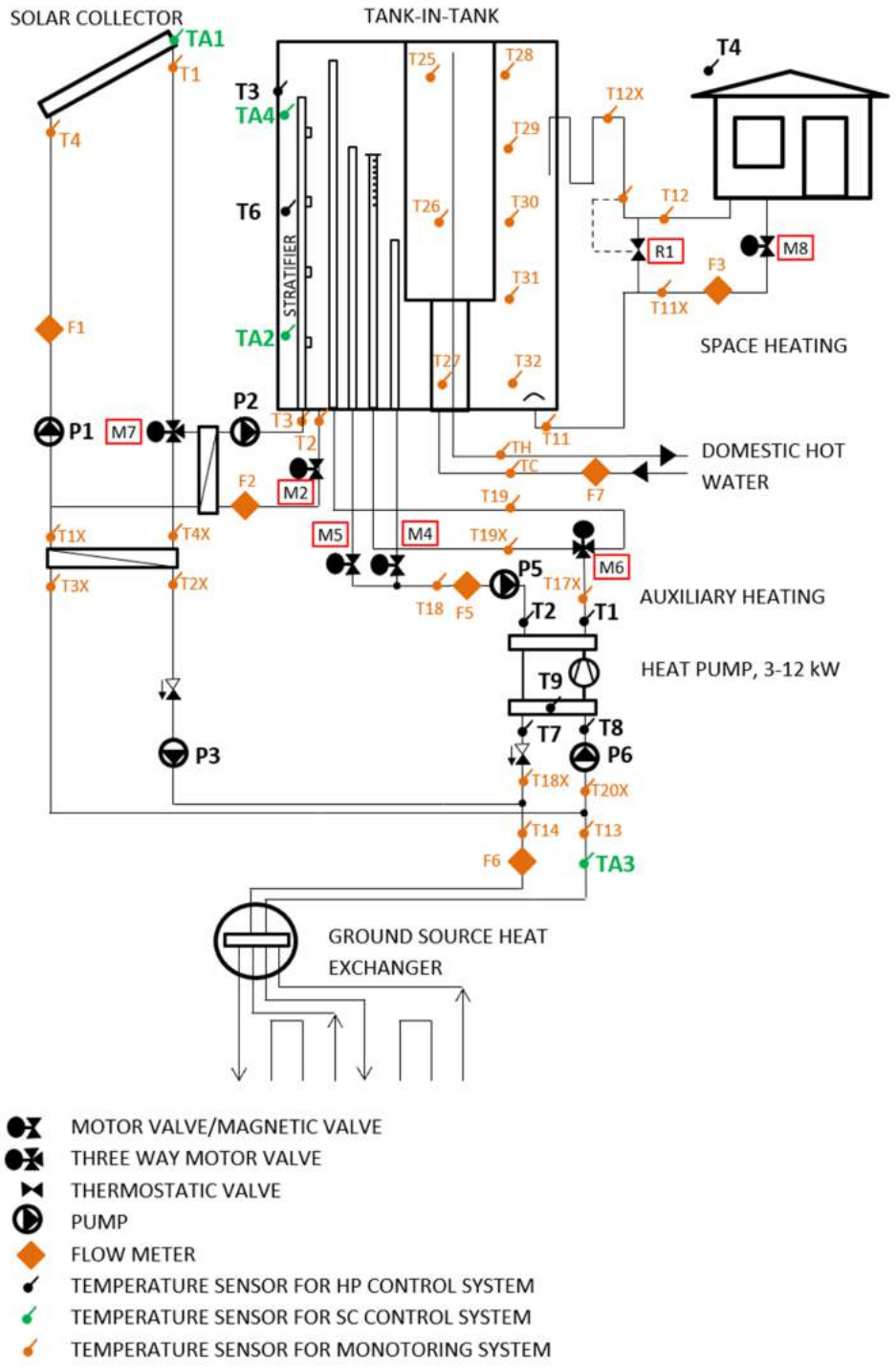

Figure 1.11: Measurement components solar heating/heat pump system [3].

Temperature sensors in storage tank	Position from bottom of storage tank [mm]
Control system	
T3	1255
T6	835
T10	320
Monitoring system	
T25	1528
T26	873
T27	231
T28	1554
T29	1233
T30	898
T31	577
T32	258

Table 1.1: Position of temperature sensors in storage tank.

Pipes in the storage tank	Upper position measured from bottom of storage tank [mm]
Auxiliary heating loop	
DHW volume inlet from HP	1400
DHW volume outlet to HP	1115
SH volume inlet from HP	1085
SH volume outlet to HP	715
Domestic hot water loop	
DHW outlet to consumer	Top of tank
DCW inlet from utility	Bottom of tank
Space heating loop	
SH outlet to consumer from SH volume	1000
SH outlet to consumer from storage tank	1250
SH inlet from consumer	Bottom of tank
Solar collector loop	
Stratification pipe	1335

Table 1.2: Position of pipes in the storage tank.

Table 1.3 shows the measurement equipment used in the primary loop of the solar collector [3].

Equipment	Type	Location	Accuracy
Flow sensor	Brunata HGS5-R4	HP-Ground loop	± 5 %
	Brunata HGQ1-R3	HP-Tank loop	± 5 %
	Brunata HGQ1-R0	Solar and SH loops	± 5 %
	Clorius Combimeter 1.5 EPD	DHW loop	± 2-3 %
Temperature sensor	Copper/constantan, type TT		± 0.5 K

Table 1.3: Measurement equipment of solar collector loop.

1.2.8 Control strategy solar collector loop

Considering the flow in the primary and secondary loop of the solar collector (pumps P1 and P2) equal to 3 l/min, solar energy is transferred to the tank according the following conditions (figure 1.11 shows the location of the different temperature sensors).

- Solar energy to the tank (First priority)
- Start: TA1 > TA2+6 K and TA1 > 20°C and TA2 < 70 °C
- Stop: TA1 < TA2+2 K
- Stop if: TA2 > 75°C,
- restart prohibited until TA2 < 70°C, TA1 > 130°C,
- restart prohibited until TA1 < 110°C

  The priority of the system is the production of DHW, the second one is the heat transfer to the ground. In the case of the second priority, pump P3 has a flow equal to 20 l/min, the operation time of this pump is 20 min with stops of 5 min to evaluate conditions of the system. The following conditions are set for the operation.

- Solar energy to the ground (Second priority) (see figure 1.11)
- Start: TA1 > TA2+8K and TA1 > 20 °C and TA3 < 30 °C
- Stop: TA1 < TA3+4 K
- Stops if TA1 > 130 °C, restart prohibited until T1 < 110 °C

1.2.9 Control strategy heat pump loop

Similar to the control strategy for the solar collector, the heat pump contains certain constrains during its operation shown below. Flow in P5 is 15 l/min, meanwhile, the flow in P6 is 20 l/min. The priorities for this subsystem are the same as the first subsystem (figure 1.11 shows the location of the different temperature sensors).

- DHW production (First priority)
- Start: T3 < 52 °C –4 K
- Stop: T3 > 52 °C
- SH production (Second priority)
- Start: T6 < 30 °C –4 K
- Stop: T6 > 30 °C

CHAPTER 2

Analysis framework

This chapter provides the general framework for the analysis of the data collected from the test facility at the Climate Station at DTU Byg. Weather conditions, volume flow rates measured in the different loops and temperatures in different measurement points of the system will be evaluated. All the data is related to the year 2019 to make a yearly assessment, the assumptions for the calculations are presented considering previous studies and scientific literature. Additionally, comparisons will be carried out taking into consideration different values of some parameters to make a further analysis of the results.

All the analysis is done considering different operational modes and weather conditions (rainy and dry periods) for specific periods during 2019. Different assumptions and limitations are stated previous to the calculations.

2.1 Analysis of the solar radiation on the solar collector

This section provides the calculation of the total solar radiation on the solar collector based on the data from the Climate Station at DTU Byg and the heat produced by the solar collector. The aim is to analyze the energy absorbed by the solar collector, the energy transferred from the solar collector to the HGSHE and to the storage tank to produce DHW or SH.

The solar collector is an evacuated tubular collector, the total transparent area is 9.6 m^2, angles of incidence for a horizontal surface (zenith angle) higher than 87 ° and lower than 90 ° are not considered in the calculations to avoid mistakes in the results. Different inputs of the collector are used for the calculations.

Considering that the climate station measures the horizontal diffuse radiation with a tracker (Module 2 channel 3) [4] and the global radiation (Module 2 channel 6) [4] during 2019, it is necessary to calculate the total solar radiation (TSR) on the sloping surface. The tilt of the solar collector is 45° oriented south 12° toward east from south. For the calculation of the TSR, it is followed the Educational note on solar radiation [1] and the calculation is done minute by minute. In terms of the energy balance in the system, the following energy quantities are used for the analysis (fig. 2.1).

- Total solar radiation on the solar collector (SC) [kWh/day].
- Energy transferred from the solar collector to the ground via an external plate heat exchanger [kWh/day] (E SC to ground).
- Energy transferred from the solar collector to the storage tank via an external plate heat exchanger [kWh/day] (E SC to tank).
- Energy provided from the ground to the heat pump via the evaporator inside the heat pump [kWh/day] (E ground to HP).

- Energy transferred from the heat pump to the storage tank via the condenser of the heat pump [kWh/day] (E HP to tank).

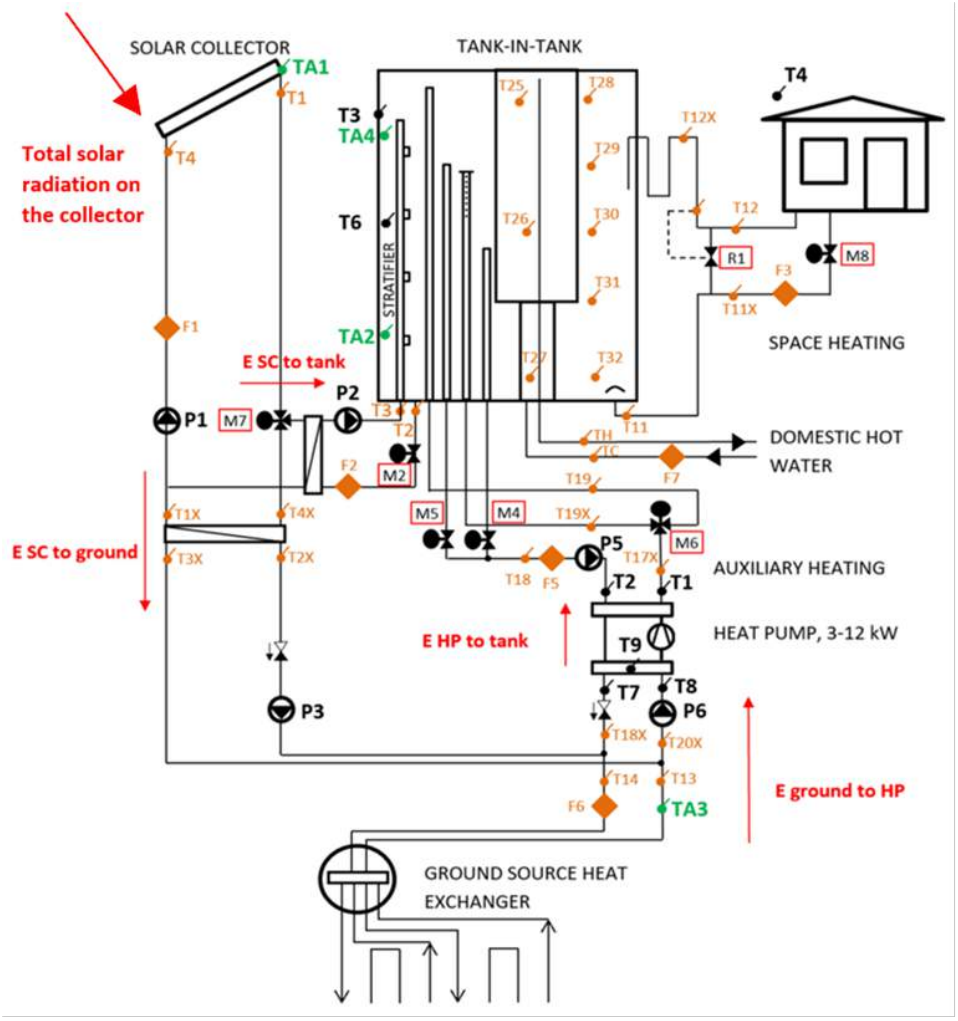

Figure 2.1: Energy flows in the system.

Additionally, the daily average air temperature and the daily rain accumulation are shown. Using the different flows of energy, the seasonal performance of the system is determined. The results are shown in monthly graphs which are useful to identify periods which there is an unusual or an unexpected condition which could indicate a malfunction of the system or missing data. For instance, it is shown the energy analysis for January and July 2019 in the figures 2.2 and A.9 respectively.

In the energy balance of January 2019, it is shown low values of total radiation on the solar collector, which is usual for this month; therefore, low values of energy is transferred to the storage tank from the SC. In terms of the heat pump operation, this operates long periods per day, and it is the main source of energy for the storage tank. The air temperature is low as it is expected, and no high rain precipitations are present during this month.

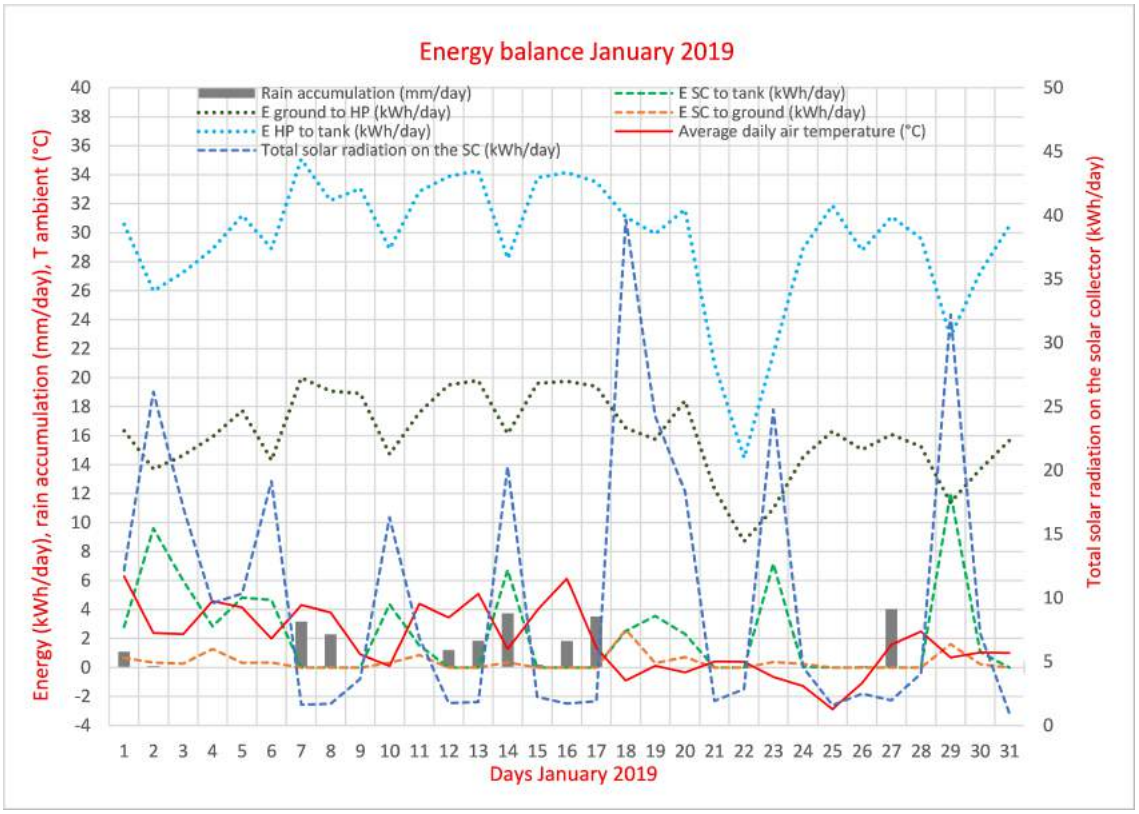

Figure 2.2: Energy balance January 2019.

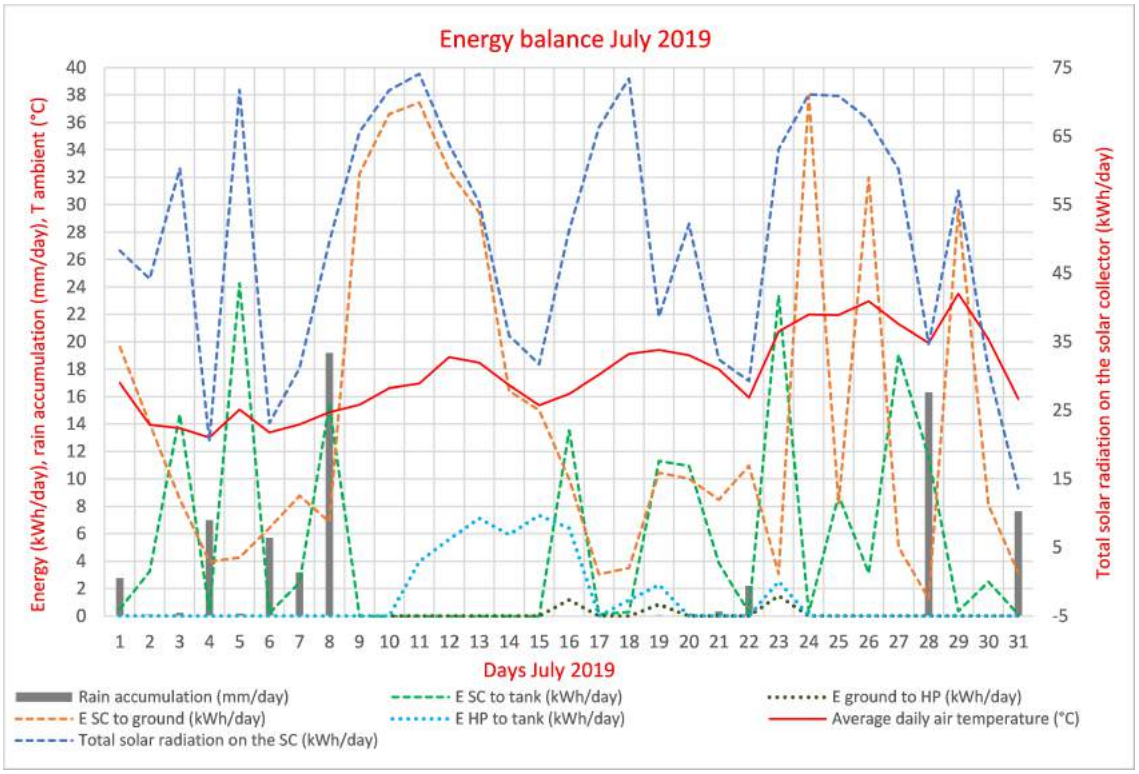

Figure 2.3: Energy balance July 2019.

The energy balance for July 2019 is quite different, high values of TSR on the SC, this means, high energy values transferred from the SC to the storage tank. It can be noticed important values of rain accumulation in some days during the month. It can be seen that

from the July 9 to 15, no energy is transferred to the storage tank even though, there are high values of TSR. Also, from the day 10 to July 17, the heat pump is in operation which is not logic since the SC could provide enough energy to the tank for production of DHW and no SH production is needed during this period. These days can be considered as not valid for the calculation of the seasonal performance due to the malfunction of the system. Checking the data, it is identified that the solar collector pump (P1) was working continuously from the day 8 until day 15. The pump P3 was working also, thus, no energy was transferred to the tank. This condition could be used to calculate the power and the heat exchange capacity rate (HECR) later since this period could be considered as a steady state condition in terms of the flow inside the HGSHE.

2.2 Analysis of the global radiation on the ground

The soil temperatures into different depths are measured with temperature sensors located beside the HGSHE. The codes of the ground sensors are $B2\_X$, where X is the depth from 1 to 10 m below the surface (Fig. 2.4).

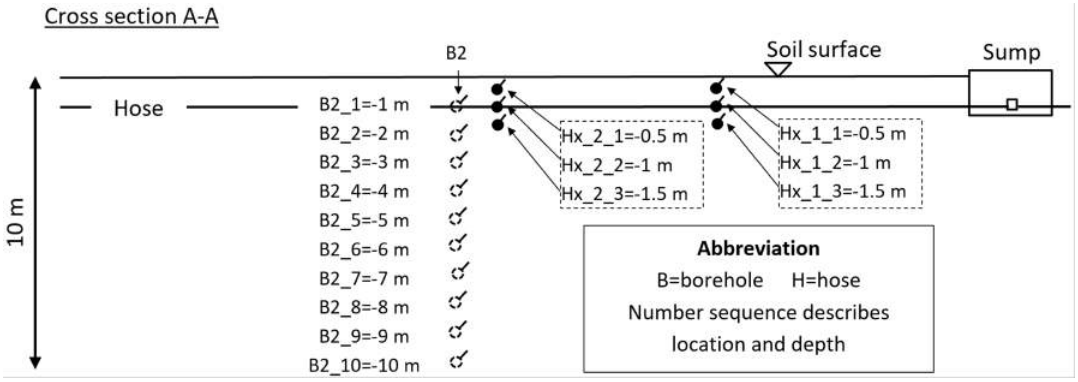

Figure 2.4: HGSHE diagram and temperature sensors location.

The analysis is done month by month to have a general assessment of the temperatures, later it will be focused on specific periods which include rainy periods or when the temperatures vary considerably. Figure 2.5 shows the analysis for July 2019, the temperature is the daily average value, the daily global radiation and the rain accumulation are shown as well. It can be noticed that the temperature 1 m below the soil (sensor B_2_1) is the most affected by the ambient conditions (global radiation, ambient temperature and rain accumulation). From 2 to 6 meters below the surface, the temperatures follow similar tendency. If the sensor is located deeper under the soil, the temperature is lower for this month, the other way around on winter months (November to March). An example is shown considering February 2019, (see fig. 2.6). It can be concluded that from 7 until 10 meters below the surface, the temperatures are very similar, considering this, it will be shown the temperatures from 1 to 6 m for the other months to have a better resolution between them.

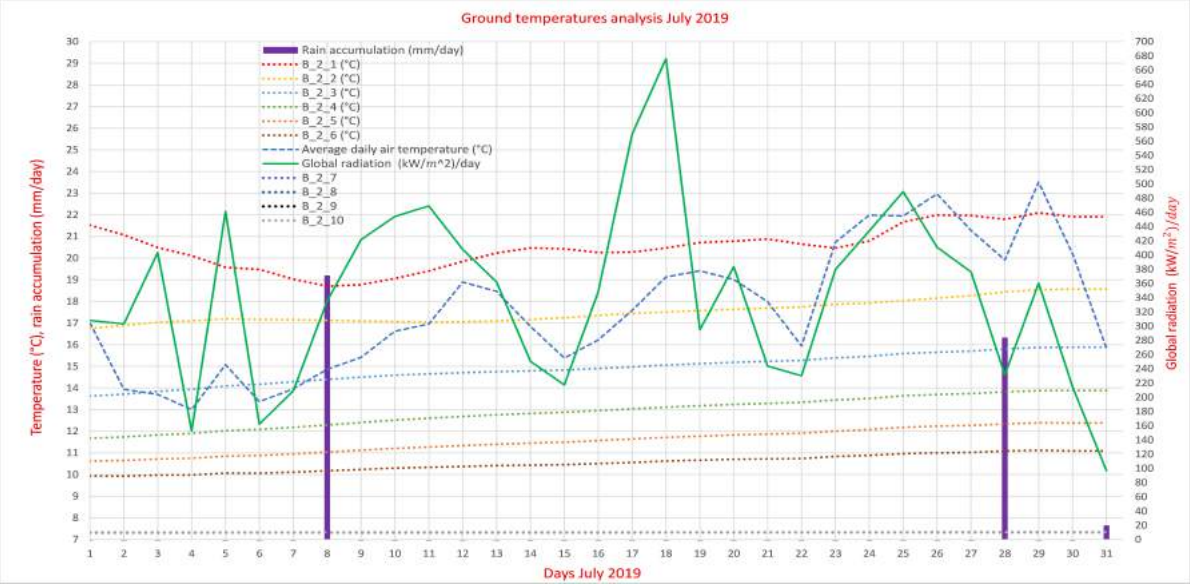

Figure 2.5: Ground temperatures analysis July 2019.

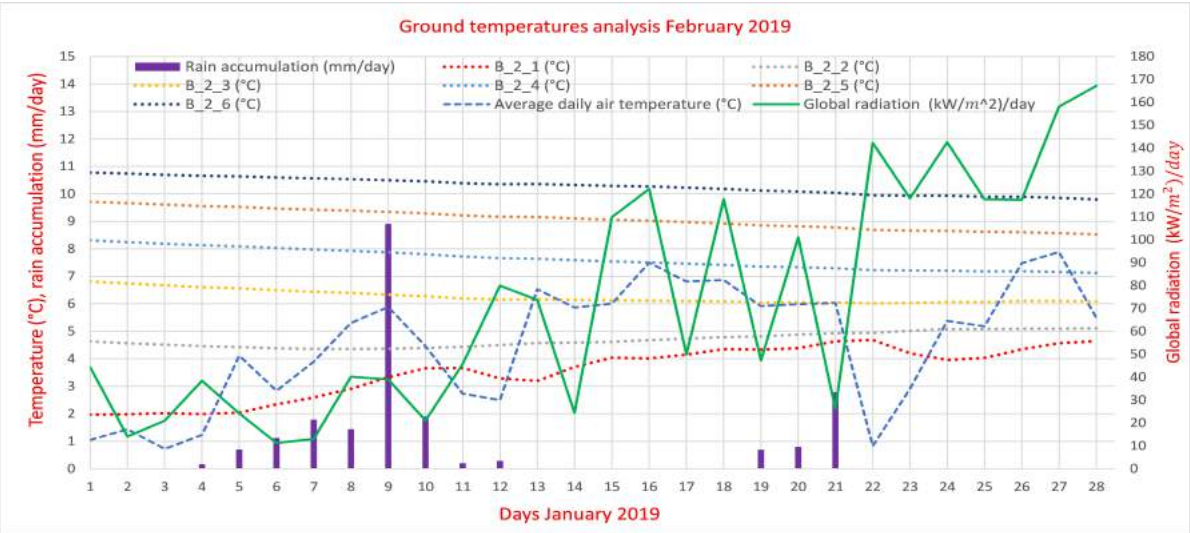

Figure 2.6: Ground temperatures analysis February 2019.

Now, the idea is to identify how the rain influences the soil temperature below the surface, for this, it is considered specific periods which there is an important rain accumulation. The aim is to determine the affectation under the ground. The chosen periods include 3 to 6 days shown in fraction day. The objective is to analyze in detail the possible temperature variations considering the delay of the changes due to the inertia of the ground.

July is a interesting month since it is a period with high global radiation values, but, also some days with important rainy periods. Figure 2.7 shows the temperature from 1 to 5 m below the soil surface, the ambient temperature, the daily global radiation (sum of the global radiation minute by minute) and the rain accumulation. Considering the period from the fifth of July until day 10, the temperature 1 m below the soil is the most affected by the change of the ambient conditions. It is shown that after a decrease of the global radiation from day 5 until day 6, the ground temperature decreases (starts at noon approximately in day 6). When

the global radiation rises enough in day 8, the ground temperature switches its tendency and increase until day 10. The delayed of the temperature tendency is related with the inertia of the ground which try to keep the current condition.

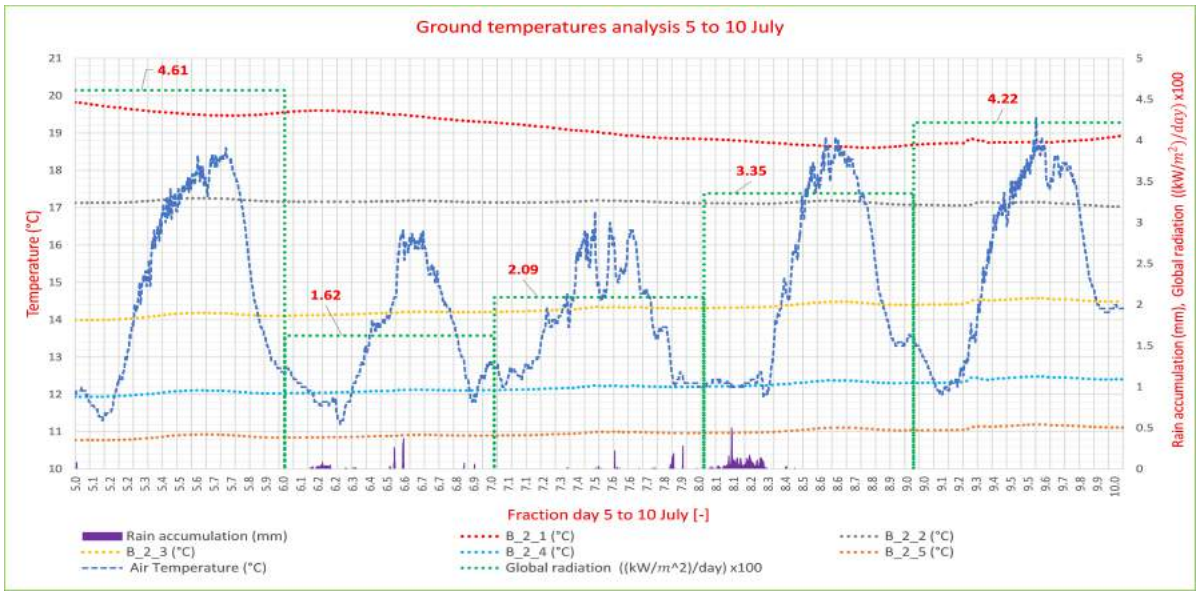

Figure 2.7: Ground temperatures analysis 5 to 10 July.

It can be seen that in presence of rainy periods, the ambient temperature decreases a certain degree (October 19, figure 2.8). For small changes on the global radiation, the change of the temperature is very small, this could be seen in the fig. 2.8. These values usually are found on winter when the global radiation is low generally.

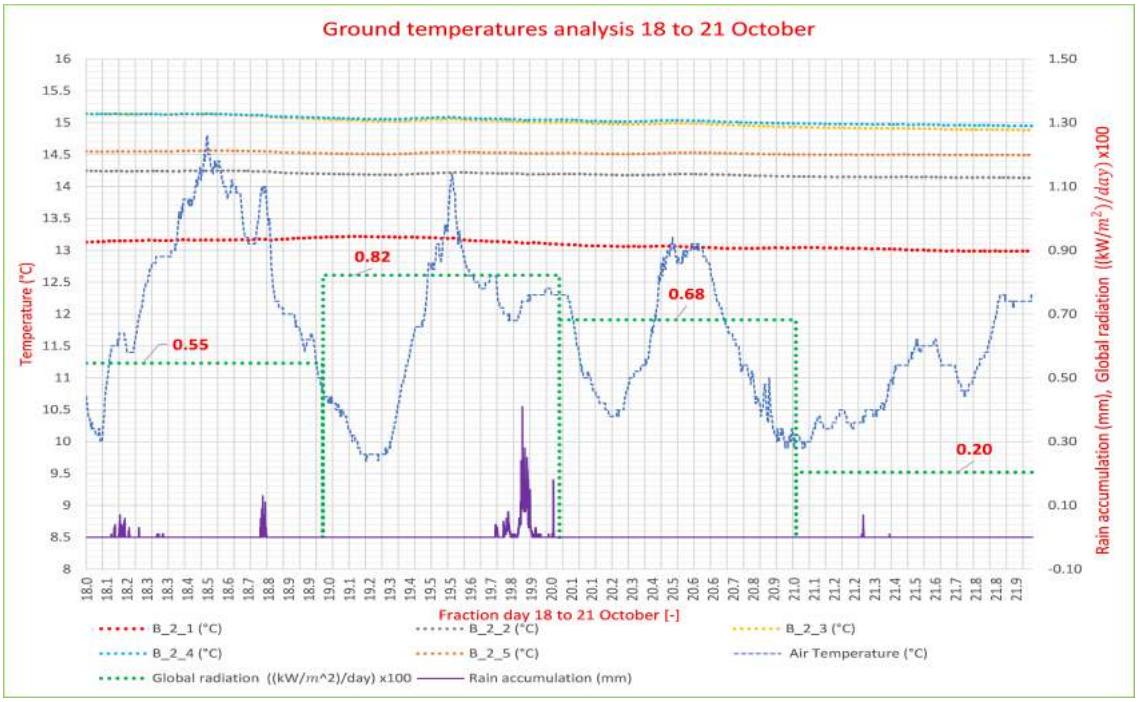

Figure 2.8: Ground temperatures analysis 18 to 21 October.

Due to the ground temperature changes over the day, it is interesting to show the distribution of the temperature at a specific time. It is selected noon as reference to show the monthly distribution of temperatures to different depths. Figures 2.9 and 2.10 show the monthly temperature at noon into different depths, from minus 1 to minus 10 m below the surface.

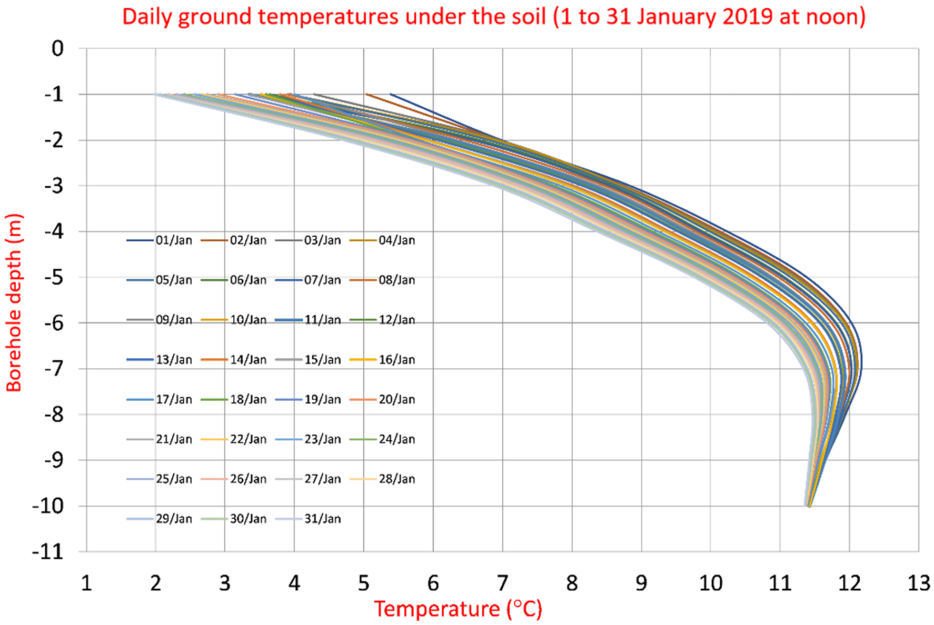

Figure 2.9: Monthly temperature at noon in different depths January 2019.

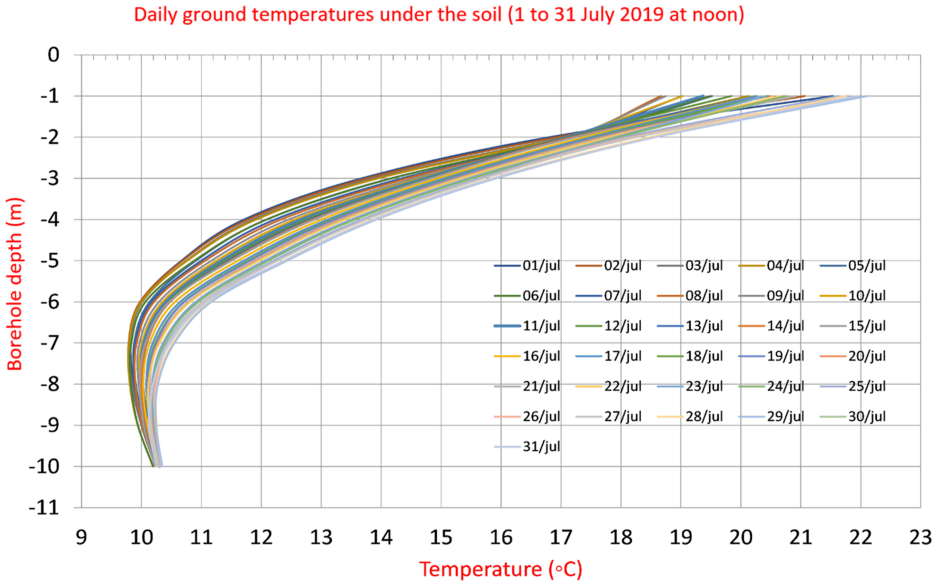

Figure 2.10: Monthly temperature at noon in different depths July 2019.

When the soil is exposed to solar radiation, part of it is reflected and the rest absorbed, increasing its temperature during part of the daytime. The temperature will then decrease during the night. When no energy input is present, the heat is transferred to the rest of the soil and/or is irradiated into the atmosphere. Soils are subjected to cycling intensity of input energy at daily or annual frequency [6]. This frequency explains why the temperature 10 m below the soil is different on January and July (approximately 1 K difference). Also, it is noticed that 10 m below the soil, the temperature is almost constant, this is due to the

thermal equilibrium between the energy absorbed by the soil and the energy emitted by this. For this reason, the lowest temperature on July 2019 at noon is around minus 7 m. Initially, the temperature decreases as the depth increases until 7 m on July for example, deeper from this, the temperature is approaching to the 10 m below the soil temperature. The other way around on winter as it can be seen in January.

2.3 Analysis on the Horizontal ground source heat exchanger (HGSHE)

Considering the initial data, it will be analyzed the relation between the inlet (T14) and outlet (T13) temperatures of the fluid inside the HGSHE, (see fig. 2.1), the ground temperatures close to the pipes and the temperatures under the soil. In addition, the cooling down and heat it up process of the ground temperatures close to the pipes (located 1 m below the soil). The ground temperature sensors locations close to each pipe are shown in the figure 2.12.

Due to the measurements are done minute by minute, it has to be analyzed 2 cases. First, considering the given data minute by minute which exists a measurement in 2 different fluid volumes inside the tubes since the fluid needs a certain time to complete a cycle around the loop. Secondly, analyzing the data which the measurements are done on the same fluid volume when this completes a cycle inside the HGSHE.

2.3.1 Calculation of a complete cycle when pump P3 is in operation.

To calculate the time which the Isopropyl alcohol (IPA) (fluid inside the HGSHE) flows through the loops (see figure 2.11), it will be analyzed a specific period which the pump P3 (see fig. 2.11) is working continuously (9 of July 2019, from 10:00 to 16:00 pm, period 1).

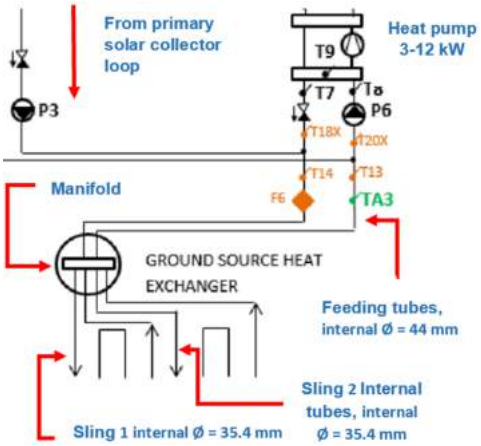

Figure 2.11: Diagram of the pipes system of the HGSHE.

The following assumptions are done for the calculations. The inputs and the results are shown in the table 2.1. Figure 2.12 illustrates the different times which are calculated during the process.

- The time zone data selection for the analysis is the Greenwich Mean Time (GMT) (GMT+0)
- As the fluid is distributed equally inside the HGSHE after the manifold into 2 slings, these must be distinguished, for this, the hose 5, 6, 7 and 8 are part of the sling 1 and the hoses 1, 2, 3 and 4 are part of the sling 2, see figure 2.12
- The flow is constant during the operation, it is equal to the average value during the analyzed period.
- The analysis is done when no energy is transferred to the storage tank.
- The total length from the manifold to the heat pump is estimated equal to 30 m.
- The analysis is done considering 2 scenarios, when the pump P3 (energy from the solar collector to the ground) is in operation and in the next section when the heat pump is in operation.

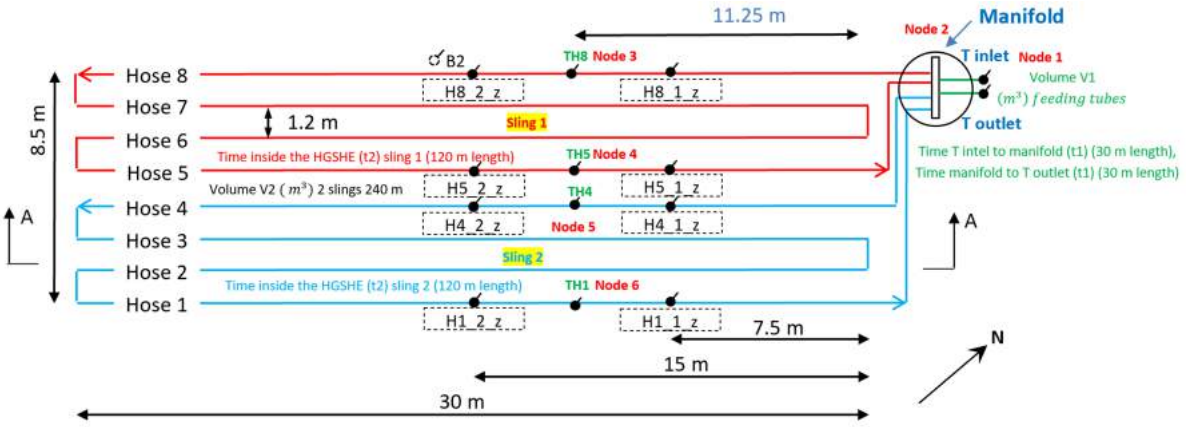

Figure 2.12: Slings in HGSHE.

The time which the fluid reaches the manifold (t1) from T14 sensor (figure 2.12) is calculated on base the diameter of the feedings tubes, the average flow (which is different for each analyzed period) and the distance between the sensor T14 and the manifold (30 m). When pump P3 is working, this time is equal to 3' approximately and around of 2' when pump P6 is working (heat pump in operation).

Parameter	Value
Internal diameter feeding tubes [m]	0.044
Internal diameter HGHE tubes [m]	0.035
Total length feeding tubes [m]	60
Total length HGHE tubes (2 slings) [m]	240
Fluid volume feeding tubes (V1) $[m^3]$	0.092
Fluid volume HGHE tubes (V2) $[m^3]$	0.236
Flow in feeding tubes and HGHE (Qf1) $[\frac{m^3}{min}]$	0.014
Time which fluid flows through feeding tubes (t1) $[t1=\frac{V1}{Qf1}]$ [min]	6.3
Time which fluid flows through HGSHE (t2) $[t2=\frac{V2}{Qf1}]$ [min]	16.3
Total time (t1+t2) [min]	22.6

Table 2.1: Complete cycle time, pump P3 in operation.

The results show that the fluid complete a cycle around the loops in 22'36". For the next step, the time which the fluid flows close to the influence area of the sensors close to the pipes are shown in table 2.2. This analysis is done to establish a better approach considering that there is an advance time in the measurements on the same fluid volume. For this calculation, the flow per sling is $Qf2$=0.007 $[\frac{m^3}{min}]$ which is half of the initial flow when the pump P3 is in operation for the period from 10:00 am to 16:00 pm July 9. Considering that the time which the fluid flows close to the influence area of the ground temperature sensors in each pipe is very similar and that the data is done minute by minute, it is established an average ground temperature per sling located in the middle between the 2 sensors, TH8 for $H8\_1\_2$ and $H8\_2\_2$ for hose 8, TH5 for $H5\_2$ and $H5\_1\_2$ for hose 5, TH4 for $H4\_1\_2$ and $H4\_2\_2$ for hose 4, TH1 for $H1\_2\_2$ and $H1\_1\_2$ for hose 1.

For the calculation is used a system of nodes (see fig. 2.12) to locate the different measurement points and facilitate the reading of the table 2.2.

Sling	Sling 1		Sling 2	
Average ground temperature per hose (8,5,4,1)	TH8	TH5	TH4	TH1
Length from manifold to temperature TH location [m]	11.25	108.75	11.25	108.75
Volume between node 2 and node 3 [1], between node 2 and node 5 [2], between node 3 and node 4 [3], between node 5 and node 6 [4] $[m^3]$	0.011 [1]	0.096 [3]	0.011 [2]	0.096 [4]
Time which the fluid reaches the nodes (node by node) figure 2.12 [min]	1.5	13.3	1.5	13.3
Time which the fluid reaches the nodes from node 2 [min]	1.5	14.8	1.5	4.8
Time which the fluid reaches the nodes from node 1 [min]	4.7	18	4.7	18

Table 2.2: System cycle time node by node, pump P3 in operation.

These times are used to establish the time ahead in the measurements related with TH8, TH5, TH4 and TH1. Of this way, we can link the temperature of the fluid and the temperature of the ground at the same time. As example it is shown in figure 2.13 how the temperatures are selected for the sling 1 in the period 9 of July.

Minute	T14 inlet (°C)	T13 outlet (°C)	(T13 outlet, t=23 min) (°C)	H8_1_2 (t=0 min) (°C)	H8_2_2 (t=0 min) (°C)	H8_1_2 (t=5 min) (°C)	H8_2_2 (t=5 min) (°C)	(TH8, t=5 min) (°C) NODE 3	H5_2_2 (t=0 min) (°C)	H5_1_2 (t=0 min) (°C)	H5_2_2 (t=18 min (°C)	H5_1_2 (t=18 min) (°C)	(TH5, (t=18min) (°C) NODE 4
1	24.48	20.74	20.6	21.088	21.649	21.099	21.672	21.3855	19.906	19.586	19.869	19.572	19.7205
2	24.44	20.74	20.6	21.091	21.654	21.101	21.67	21.3855	19.899	19.586	19.867	19.572	19.7195
3	24.41	20.72	20.6	21.094	21.662	21.092	21.665	21.3785	19.892	19.581	19.867	19.574	19.7205
4	24.36	20.71	20.6	21.098	21.669	21.093	21.658	21.3755	19.886	19.578	19.867	19.576	19.7215
5	24.38	20.69	20.61	21.099	21.672	21.093	21.66	21.3765	19.879	19.575	19.871	19.578	19.7245
6	24.44	20.68	20.61	21.101	21.67	21.096	21.668	21.382	19.876	19.574	19.876	19.581	19.7285
17	24.79	20.59	20.69	21.206	21.828	21.214	21.816	21.515	19.866	19.572	19.928	19.622	19.775
18	24.78	20.59	20.68	21.223	21.845	21.209	21.809	21.509	19.869	19.572	19.928	19.623	19.7755
19	24.66	20.59	20.68	21.22	21.833	21.201	21.796	21.4985	19.867	19.572	19.927	19.623	19.775
20	24.55	20.59	20.68	21.215	21.819	21.193	21.779	21.486	19.867	19.574	19.929	19.623	19.776
21	24.56	20.6	20.69	21.214	21.816	21.19	21.777	21.4835	19.867	19.576	19.933	19.625	19.779
22	24.6	20.6	20.7	21.209	21.809	21.19	21.774	21.482	19.871	19.578	19.935	19.63	19.7825
23	24.63	20.6	20.71	21.201	21.796	21.197	21.779	21.488	19.876	19.581	19.944	19.634	19.789

Figure 2.13: Selection of time ahead for ground temperatures for sling 1.

2.3.2 Calculation of a complete cycle when pump P6 is in operation

The same analysis is carried out considering the case when the heat pump is in constant operation (pump P6) for a representative period, the selected period belongs to January 15 from 04:34 to 06:18 am, period 2. The different here is that the flow in P6 which is much bigger than the P3 flow, in this case, Qfp=0.021 $[\frac{m^3}{min}]$, this value is the average in the period. The inputs and results are shown in table 2.3.

Parameter	**Value**
Internal diameter feeding tubes [m]	0.044
Internal diameter HGHE tubes [m]	0.035
Total length feeding tubes [m]	60
Total length HGHE tubes (2 slings)[m]	240
Fluid volume feeding tubes (V1) $[m^3]$	0.092
Fluid volume HGHE tubes (V2) $[m^3]$	0.236
Flow in feeding tubes and HGHE (Qfp) $[\frac{m^3}{min}]$	0.021
Time which fluid flows through feeding tubes (t1) $[t1=\frac{V1}{Qf1}]$ [min]	4.4
Time which fluid flows through HGSHE (t2) $[t2=\frac{V2}{Qf1}]$ [min]	11.2
Total time (t1+t2) [min]	15.6

Table 2.3: Complete cycle time, heat pump in operation.

When the flow is bigger, the time will decrease across the HGSHE, 15'36" in this case, thus, the time when the fluid reaches the reference nodes located close to the pipes will be lower also. For this calculation, half of the flow is used $Qfp1$=0.011 $[\frac{m^3}{min}]$ and the different times are shown in table 2.4

Sling	Sling 1		Sling 2	
Average ground temperature per hose (8,5,4,1)	TH8	TH5	TH4	TH1
Length from manifold to temperature TH location [m]	11.25	108.75	11.25	108.75
Volume between node 2 and node 3 [1], between node 2 and node 5 [2]„ between node 3 and node 4 [3], between node 5 and node 6 [4] $[m^3]$	0.011 [1]	0.096 [3]	0.011 [2]	0.096 [4]
Time which the fluid reaches the nodes (node by node) figure [min]	1.1	9.1	1.1	9.1
Time which the fluid reaches the nodes from node 2 [min]	1.1	10.2	1.1	10.2
Time which the fluid reaches the nodes from node 1 [min]	3.2	12.4	3.2	12.4

Table 2.4: System cycle time node by node, heat pump in operation.

2.4 Analysis of Temperatures on the HGSHE

2.4.1 Temperatures analysis, solar collector in operation

This section covers a preliminary analysis related to the temperatures close to the pipes, inlet (T14), outlet (T13) temperatures of the fluid and the temperature in the sensor B_2_1 (Tground). Figure 2.14 shows the temperatures during the period 1 minute by minute and the respective time ahead when the pump P3 is operating. The following assumptions were done for the calculations:

- The ground temperature sensors close to hose 8 and 5 corresponds to the sling 1 ($H8\_1\_2$, $H8\_2\_2$, $H5\_2$ $H5\_1\_2$), (Fig. 2.12). TH8 (hose 8) and TH5 (hose 5) are the average ground temperatures close to each hose.
- The ground temperature sensors close to hose 4 and 1 corresponds to the sling 2 ($H4\_1\_2$, $H4\_2\_2$, $H1\_2\_2$, $H1\_1\_2$, (Fig. 2.12). TH4 (hose 4) and TH1 (hose 1) are the average ground temperatures close to each hose.
- The soil temperatures beside the slings are equal to the average temperature of TH8 and TH5 for sling 1 (Tg1) and TH4 and TH1 for sling 2 (Tg2).
- The analysis is done considering the data minute by minute and the time ahead calculated in the previous section for both operational modes (P3 and P6 in operation).
- The temperature measured by the sensor B_2_1 (Tground) is considered as the temperature of the ground.
- The first 3 minutes of operation of the pump are disregarded considering that they could show invalid data for the analysis.

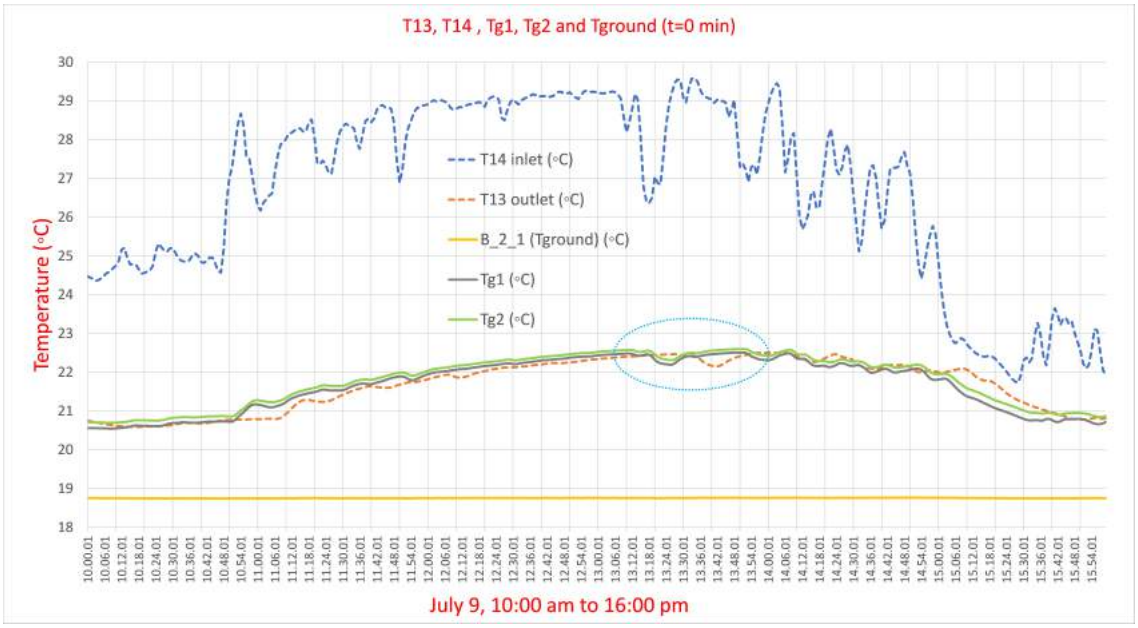

Figure 2.14: Temperatures HGSHE t=0 min, pump P3 in operation July 9.

Figure 2.14 shows the temperatures distribution on July 9 for the period 1. T13 has a similar shape as the ground temperatures close to the slings (Tg1 and Tg2), thus, it can be stated that the temperature of the surroundings around the pipes is very influenced by the temperature of the fluid. Also, it can be noticed a gap between T13, Tg1 and Tg2 (light blue

dotted line), this represents the time ahead in the calculations on the same fluid volume. In terms of the T14, this increases during the morning and decreases in the afternoon as usually does on July. Considering the sensor B_2_1, this measures a constant temperature during the analyzed period, thus, the temperature beside the HGSHE is not influenced by the process.

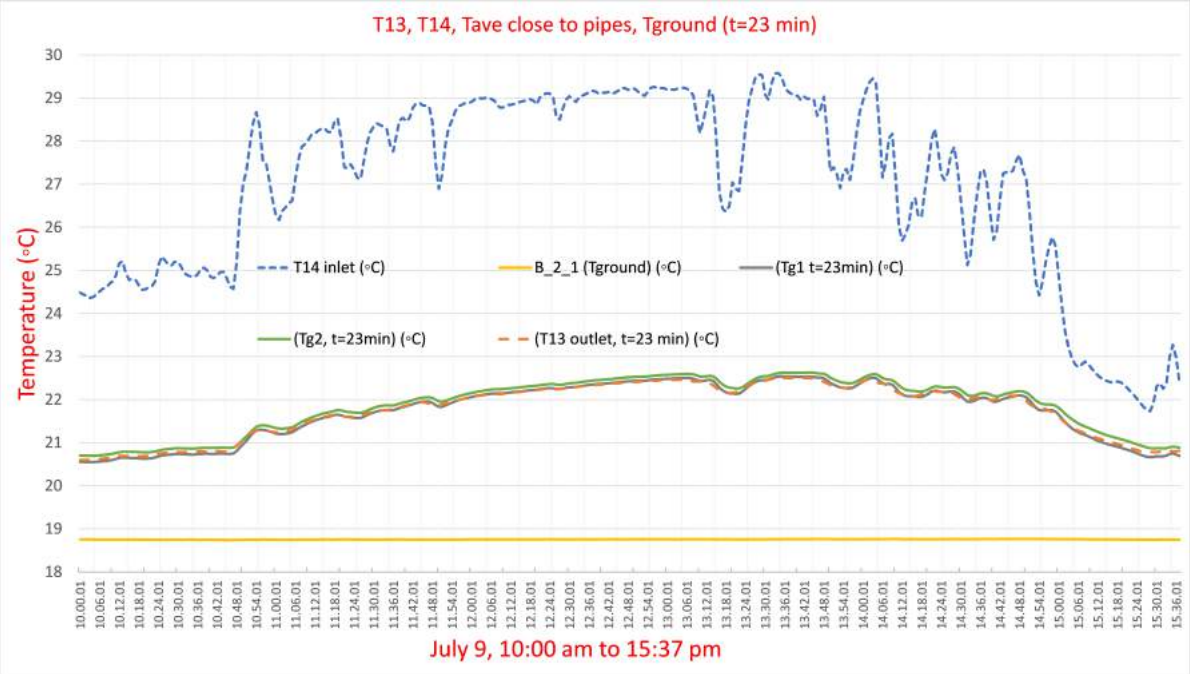

Figure 2.15: Temperatures close to the pipes t=23 min July 9.

When the gap is corrected (fig. 2.15), the shape of T13 almost fits with Tg1 and Tg2, this means that the initial approach for the time delayed in the first scenario is pretty accurate (22'36"). Since the data is given minute by minute and the calculated time is 22'36", it is chosen the value equal to 23' which fits better in this analysis. If the value 22' is chosen, the figure would show that T14 reacts before T13 which is not logical since T14 is the input in the analysis.

Furthermore, it is used the calculated time values to correct the gap of the ground temperatures TH8, TH5, TH4 and TH1 (table 2.2). Those measurements are graphed for the period 1(fig. 2.16) and it could be noticed that TH8 and TH4 vary a little. In theory they should have the same value since it is the first measurement point in the analysis for sling 1 and sling 2 respectively (see fig. 2.12). This behavior has more than one reason, one explanation could be related with the accuracy of temperature sensors ($\pm$ 0.5 K). Another reason is related with the location of the sensors under the ground which is different sensor by sensor. For this period, T14 is higher than TH8 and TH5, thus, heat is transferred to the soil. T13 is higher than TH5 an TH1, so, the process continues until the fluid returns to the feeding tubes. This is a discharging process which heat is transferred to the ground, if heat is transferred to the fluid, it will be a charging process.

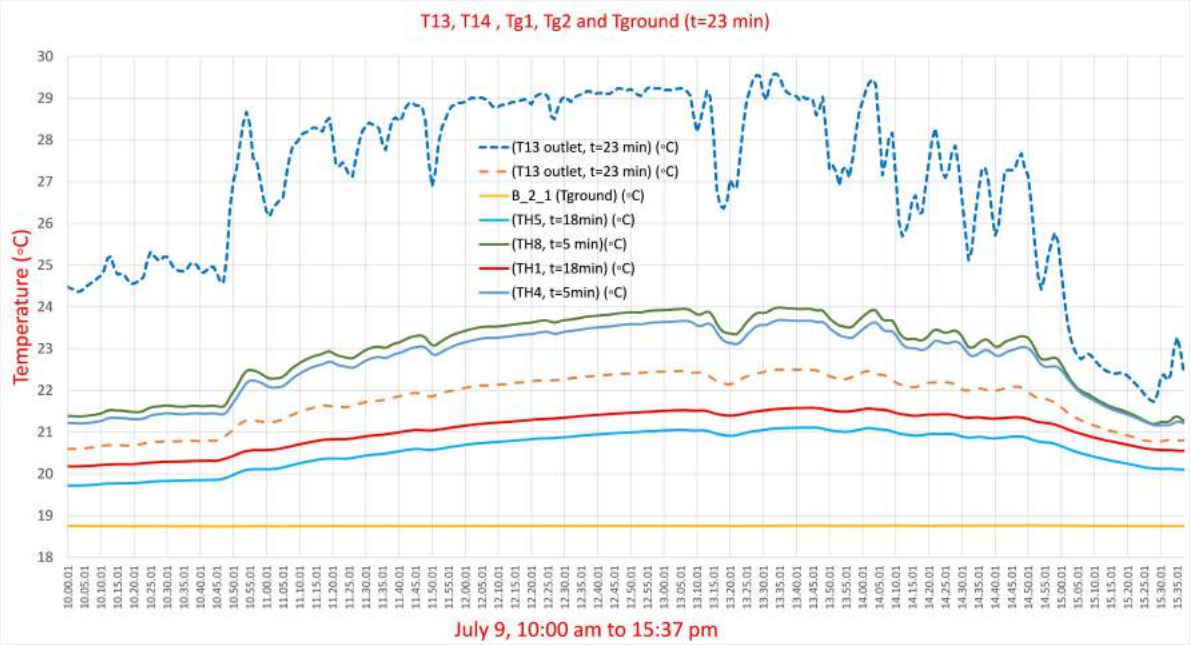

Figure 2.16: Temperatures HGSHE t=23 min, pump P3 in operation July 9.

For a complete day analysis when P3 is working continuously (see fig.2.17), it can be noticed that all the temperatures are very similar during the night, increasing the their values during the day until noon and decreasing in the afternoon. The Tground is almost constant during all day.

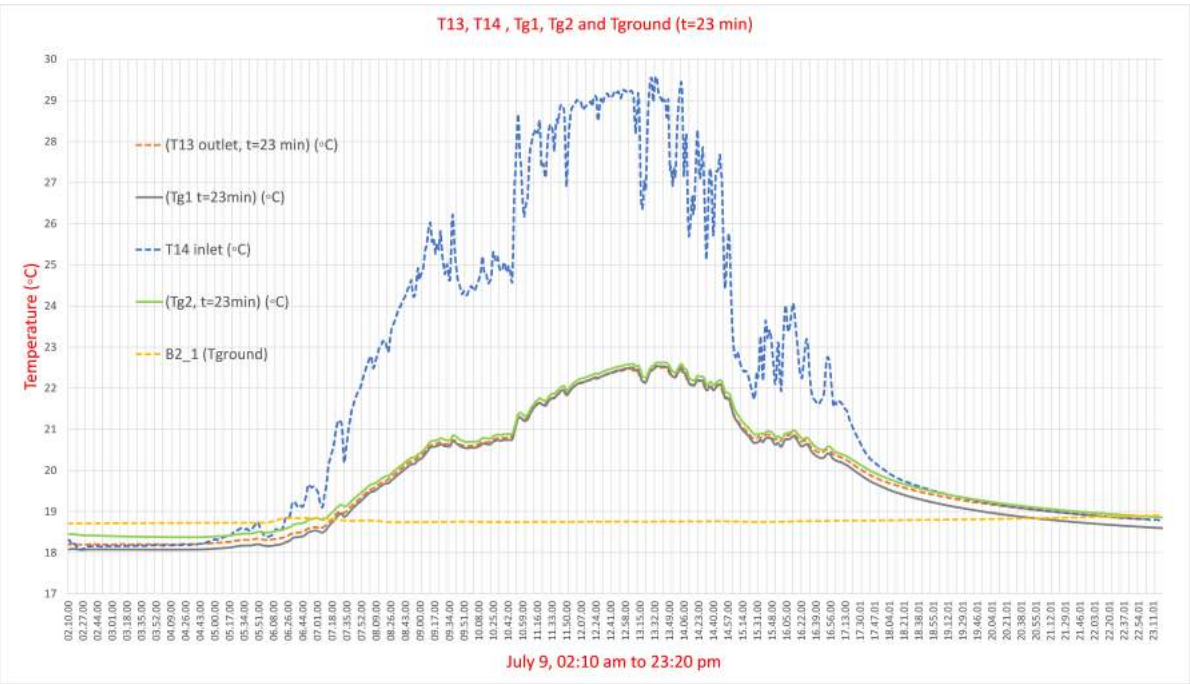

Figure 2.17: Temperatures analysis 9 July.

Figure 2.18 shows similar temperature features as the previous analysis. It can be seen that T14 has up and downs during all the period, the reason for this is linked to the operational mode of the pump P3 which stops for short periods. These stops are used to evaluate the conditions of the system, if the changes are not significant after the evaluation of the conditions,

P3 starts working again. Short periods like these are considered not too large to change the stability of the system, the stops time which the pump P3 was not in operation (2 or 3 min) it not included in the analysis. Another difference in comparison with the previous analysis is the time ahead calculated, for this period, the time which fits better is 22'.

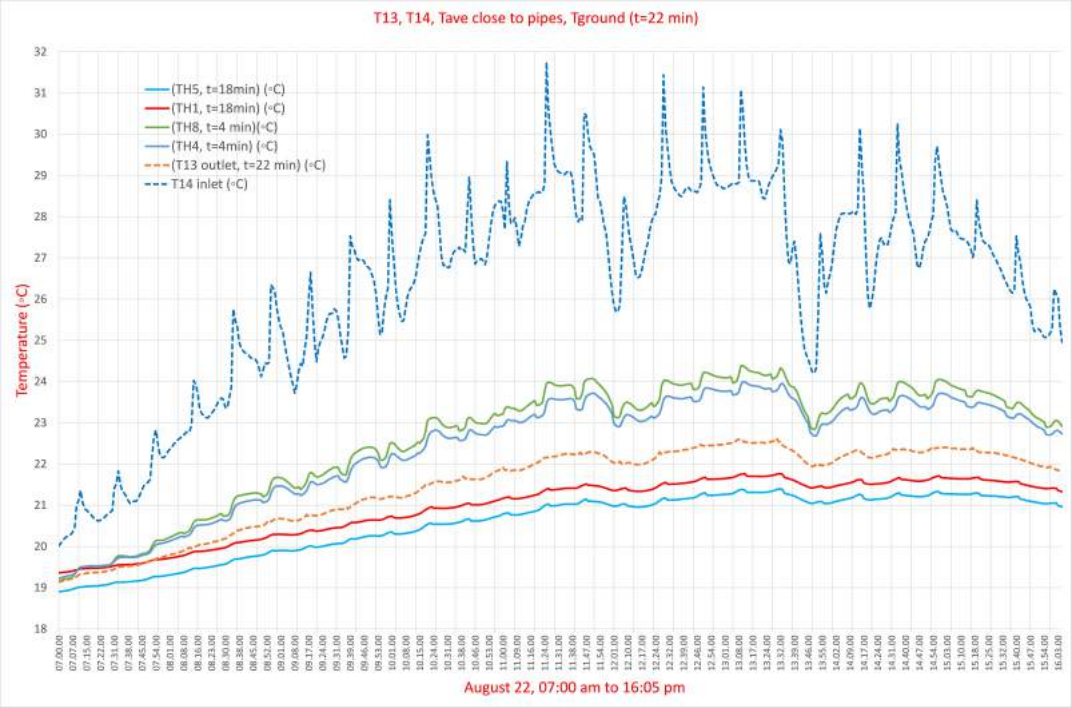

Figure 2.18: Temperatures analysis 22 August 2019.

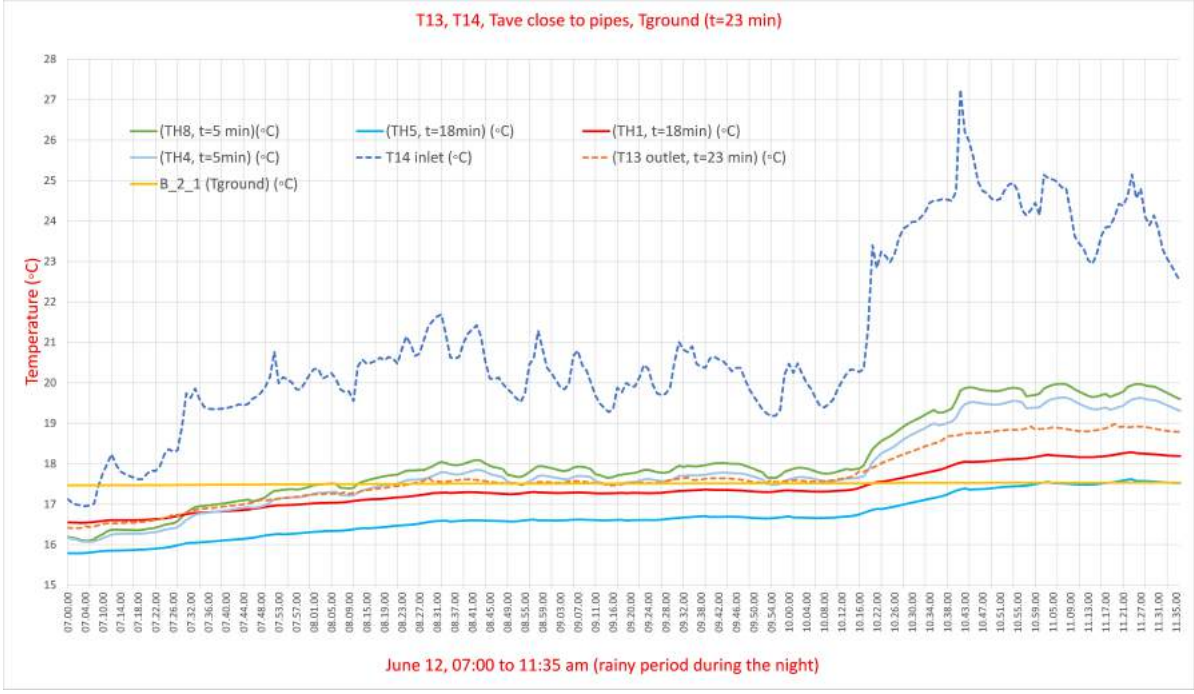

Figure 2.19: Ground temperature analysis, June 12 (rainy period).

An additional study is related with the case which there is a rainy condition. Considering

the period June 12 2019 (07:00 to 11:36 am), rainy period from 02:00 to 04:30 am (5.43 mm of rain fall in total using a cumulative accumulation after the latest auto reset). Figure 2.19 shows a different tendency on the temperatures close to the pipes. For the sling 1, the temperatures TH8 and TH5 keep a very similar tendency. On the other hand, TH4 and TH1 in sling 2 present a different tendency. Due to the accuracy of the temperature sensors, it is difficult to state a conclusion about the degree of the affectation since the temperature difference is below 0.5 K for both cases.

2.4.2 Heat pump loop in operation

Similar to the previous section, it will be analyzed the case which the heat pump is in operation (pump P5). The analyzed period is on January 27 from 09:30 to 10:50 am (fig. 2.20). The same initial conditions are used for this scenario and 2 cases will be evaluated. First, minute by minute and considering the time ahead calculated previously for this operational mode (January 15).

Figure 2.20: Temperatures HGSHE t=0 min, Heat pump in operation January 27.

Figure 2.20 shows a charging process when heat is transferred to the fluid from the ground. After this, the heat is transferred from the Isopropyl alcohol (IPA) to the coolant of the heat pump (R134a). Finally, the heat pump will supply heat to produce DHW or SH according to the needs of the system. The priority of the system is the production of DHW. As soon as the pump starts to operate, more heat is transferred from the fluid inside the evaporator of the heat pump, thus, T14 decreases. At some point, T14 droops sharply and T13 follows the tendency. Checking the data, it is noticed that at this point, the heat pump starts to provide heat for the production of space heating. This can be seen analyzing the values of the sensor T30 in the storage tank (see fig.2.1).

Considering the initial time calculated for a complete cycle of the fluid inside the HGSHE in this operational mode (15'36"), it is seen that for this period, the optimal time is equal to 13 min. A bigger average flow and short analyzed periods contribute to this difference. Figure 2.21 shows the analysis without the time delayed in the measurements, one more time it is noticed that the ground temperatures close to the pipes are influenced by the fluid temperature. Figure 2.22 shows the temperatures close to each pipe, it is seen that T13 is very similar to TH5 and TH1 as it was expected.

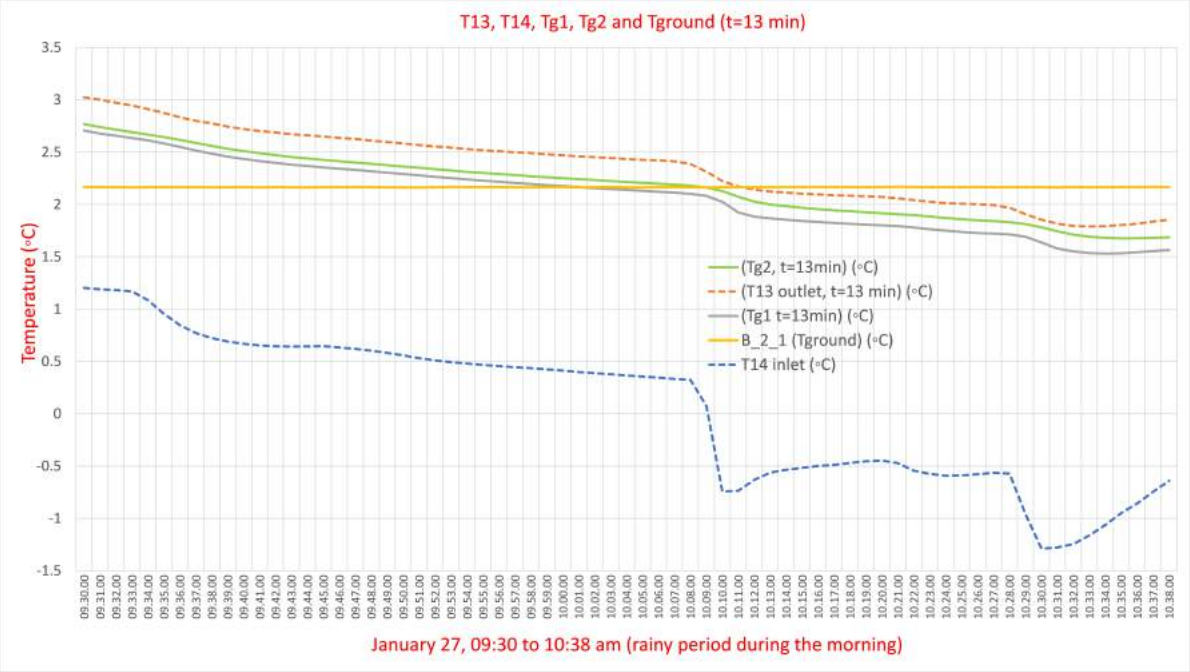

Figure 2.21: Temperatures HGSHE t=13 min, Heat pump in operation January 27.

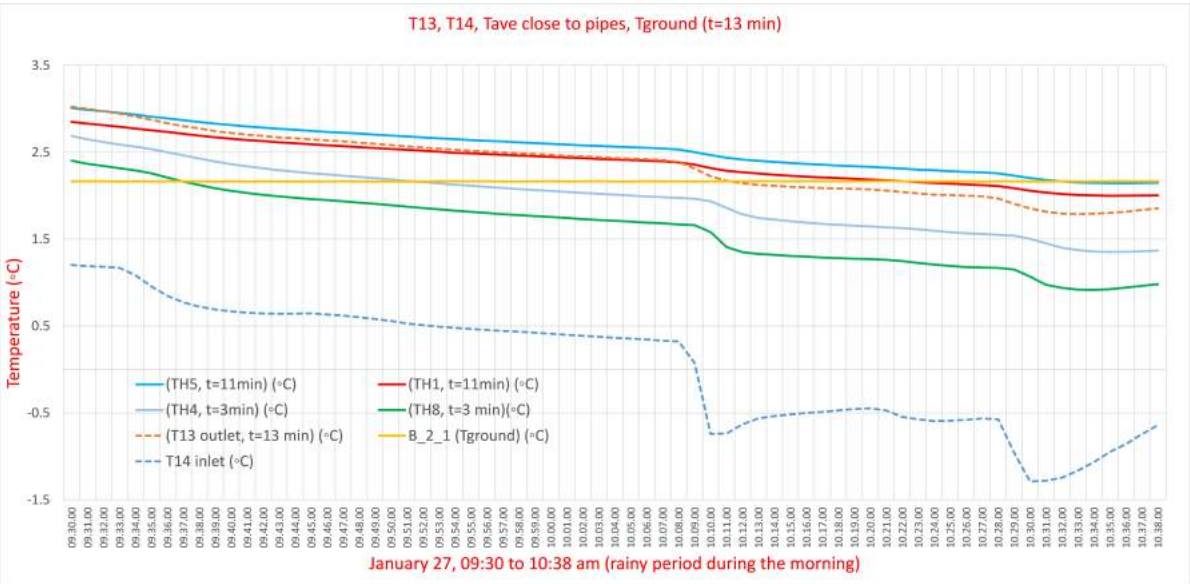

Figure 2.22: Ground temperatures close to the pipes, January 27.

2.5 Analysis of the Heat exchange capacity rate (HECR) and Power

The calculation of the Heat exchange capacity rate (HECR) will state how large power can be transferred from the fluid (IPA) inside the HGSHE to the soil per K temperature difference between the soil and the IPA when the solar collector is operating. The same analysis will be done when the heat pump is in operation. The time delayed is considered for the different calculations to have accurate results. For example, the time which the fluid flows from node 1 to node 3 (5 min for July 9) (see figure 2.23 must be taken as reference to select the time ahead for the ground temperature in node 3 (sensor $H8\_1\_2$). That means, select the measurement in the minute 5 for this sensor in order to evaluate the influence of the temperature fluid on the ground (see fig. 2.13).

2.5.1 Calculation of Power

For the calculation of Power, some inputs are needed. In terms of the fluid inside the HGSHE, it is considered a density [ρ] and the heat capacity [Cp] as constant values (ρ=892 and Cp=3400) to simplify the analysis. It is also considered an average volume flow [$\dot{V}$] inside the HGSHE. For these analysis, constant operation periods with stops no longer than 3 min will be evaluated. ΔT is the difference between T13 and T14.

The power is defined as:

$$Power[W] = \dot{V} * \rho * Cp * \Delta T \tag{2.1}$$

2.5.2 Calculation of the Heat Exchange capacity rate (HECR)

To evaluate the HECR between the fluid and the soil close to the pipes are considered the following assumptions:

- The pipes in the feeding tubes are well insulated, therefore, the following assumptions are done for the sling 1. T14 is considered constant from node 1 to node 3 (see Fig. 2.23), in terms of T13, it is considered constant from node 4 to node 7. For the sling 2, T14 is constant between node 1 and node 5 and T13 constant between node 6 and node 7.

- The mean temperature between the soil temperature close the pipes and the temperature of the fluid is calculated following the logarithmic mean temperature difference (LMTD) equation 2.3.

- The HECR is calculated in sling 1 and 2. In addition, it is used the average LMTD of both slings to calculate an average HECR for the HGSHE.

- It is calculated the time ahead between the different nodes to make a better approach of the calculation. This means, the time which the fluid flows close the node 3 and 4 in sling 1. The same calculation when the fluid flows close to node 5 and 6 for the sling 2.

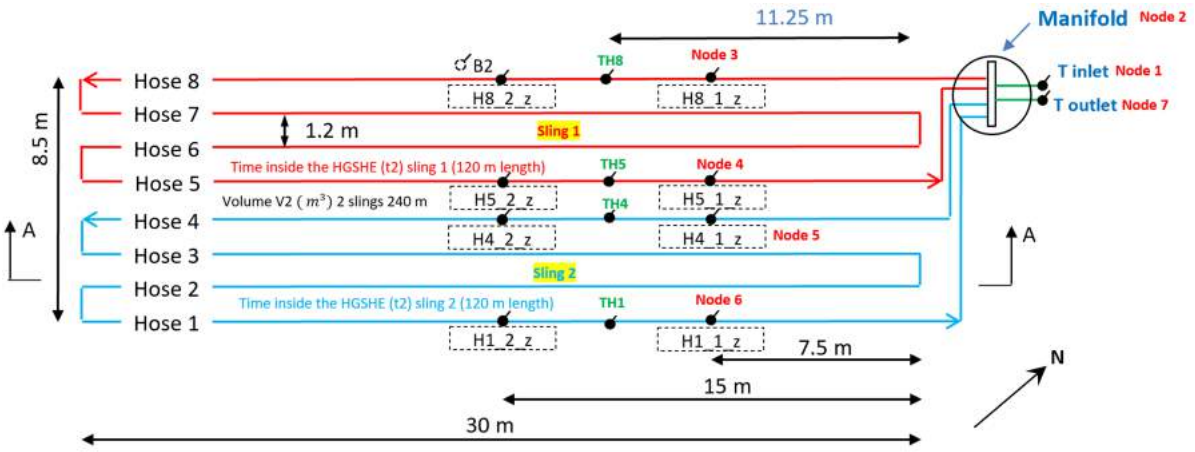

Figure 2.23: Nodes diagram HGSHE.

The HECR is defined as:

$$HECR = \frac{Power}{\Delta T_m} \tag{2.2}$$

Where ΔT_m is the LMTD is represented in 2.3 for sling 1.

$$\Delta T_m = \frac{\Delta T(node5) - \Delta T(node8)}{\ln \frac{\Delta T(node5)}{\Delta T(node8)}} \tag{2.3}$$

The different values of ΔT are result of the difference between the temperature of the fluid and the temperature of the ground close to the pipes measured by the sensor in the different nodes (Fig. 2.23). For example, ΔT (node 8)= T14 - T($H8\_1\_2$). Figure 2.24 shows the power and the HECR for the period Jul 9 (10:00 am to 15:37 pm). To compare T13 and its influence on the ground, it is established the time ahead in the measurement as it was done in table 2.13. The same for the other temperature sensors close to the ground included in the analysis.

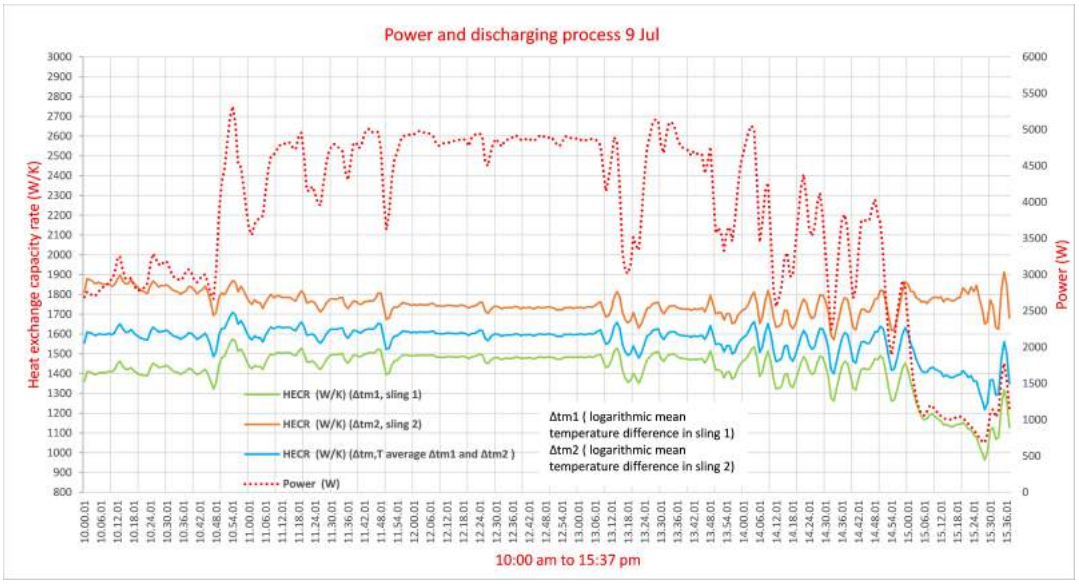

Figure 2.24: Power and HECR, July 9.

Due to the difference between the ground temperatures close to the pipes, the HECR is different for each sling. An average of 1750 $\frac{W}{K}$ for the sling 1 and 1500 $\frac{W}{K}$ for the sling 2. In terms of the Power, this changes during the day as it was expected, when T14 is constant for a short period (around 12:09 until 13:00 pm), the Power is around 2600 W. This analysis is carried out when the solar collector loop is in operation. Figure 2.25 shows the same analysis when the heat pump is working on January 27. The results show different values, a Power equal to 5500 W at the beginning of the analysis increasing rapidly when the production of space heating water occurs and a average HECR value of around 4500 $\frac{W}{K}$, decreasing its value when the production of space heating water occurs inside the storage tank.

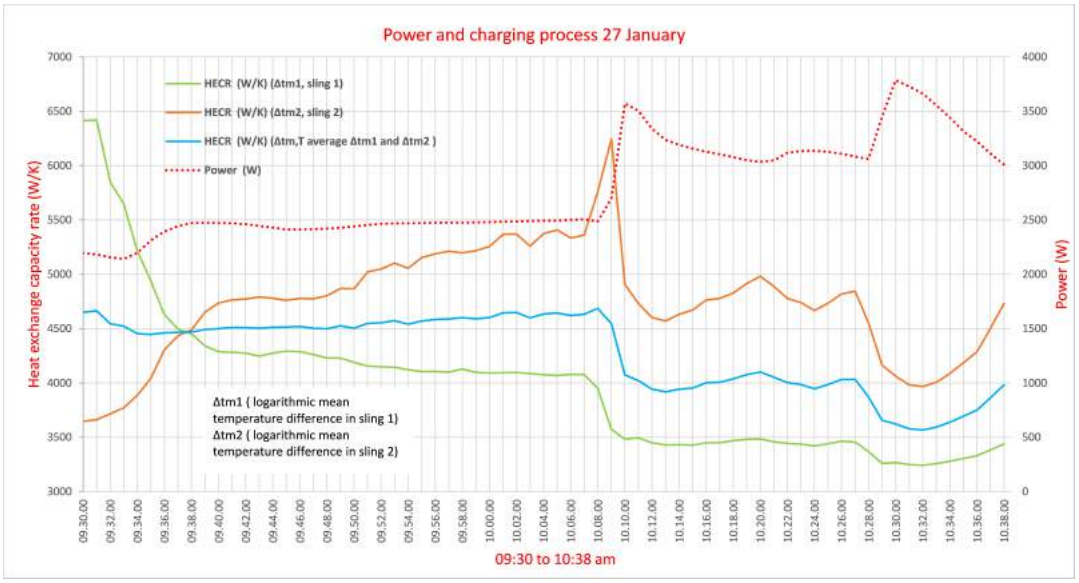

Figure 2.25: Power and HECR, January 27.

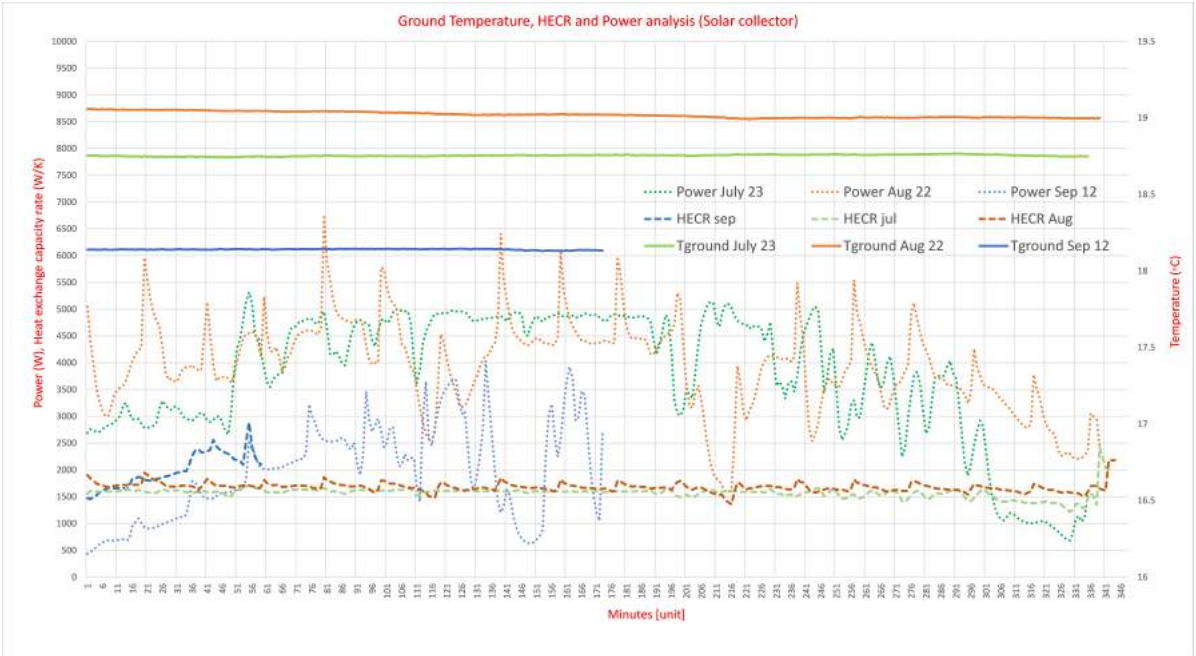

Figure 2.26: Analysis Tground, Power and HECR, SC in operation.

Due to the considerations for the calculation of the Power generated in the process (ρ and

Cp constant values), it is noticed that this depends of the ΔT of the fluid and the $\dot{V}$. In each operational mode, the $\dot{V}$ is almost constant, thus, the main parameter which influences the power is the temperature different of the fluid (T14 and T13). Figures 2.26 and 2.27 shows the relationship between the soil temperature, Power and the average value of the HECR for both operational modes.

Figure 2.27: Analysis Tground, Power and HECR, HP in operation.

Since the calculations were done in different hours in these days, the analysis is presented in minutes, Power is higher when the temperature of the soil is higher, this is characteristic on summer months. Tground tends to keep its current temperature, so, the difference between T14 and Tground is higher on summer periods. In terms of the HECR, the results show the opposite, the HECR is slightly higher when the temperature of the soil is lower. For July 9 and August 22, the average value of the HECR is almost the same since Tground in both cases is very similar. When the heat pump is in operation, the figure 2.27 shows a different tendency due to these are very sensitive to the inputs.

CHAPTER 3

Simulation on TRNSYS

In this chapter is presented a model of the HGSHE on Transient System Simulation Tool (TRNSYS). The aim of the simulation is to determine the pipe soil contact resistant (PSCR) value in order to calculate an outlet temperature (T13 C) as close as possible to the measured outlet temperature (T13 M). The simulation is focused on 2 operational modes, energy is transferred from the solar collector to the ground (discharging process) and energy is transferred from the ground to the heat pump (charging process). Due the the complexity of the analysis when the solar collector loop and the heat pump loop are in operation simultaneously, this scenario is not considered in the analysis.

3.1 HGSHE TRNSYS model

The HGSHE on TRNSYS is type 997, this is a horizontal ground heat exchanger which layers of horizontal pipes can be set from 1 or more levels. In the analyzed case, the value is equal to 1 layer. A specific fluid circulates through the HGSHE providing heat to the soil or absorbing heat if this is a charging process. The HGSHE pipes are spaced 1.2 m between each of them and it is located 1 m under the surface. Different heat transfer processes occur in the soil-pipes system , conduction between the pipes, walls and the soil, a convection process inside the pipes. In terms of the soil, heat transfer from the soil surface to the surroundings occurs by radiation and convection. Figure 3.1 shows a 2D sketch of the boundary conditions for the HGSHE.

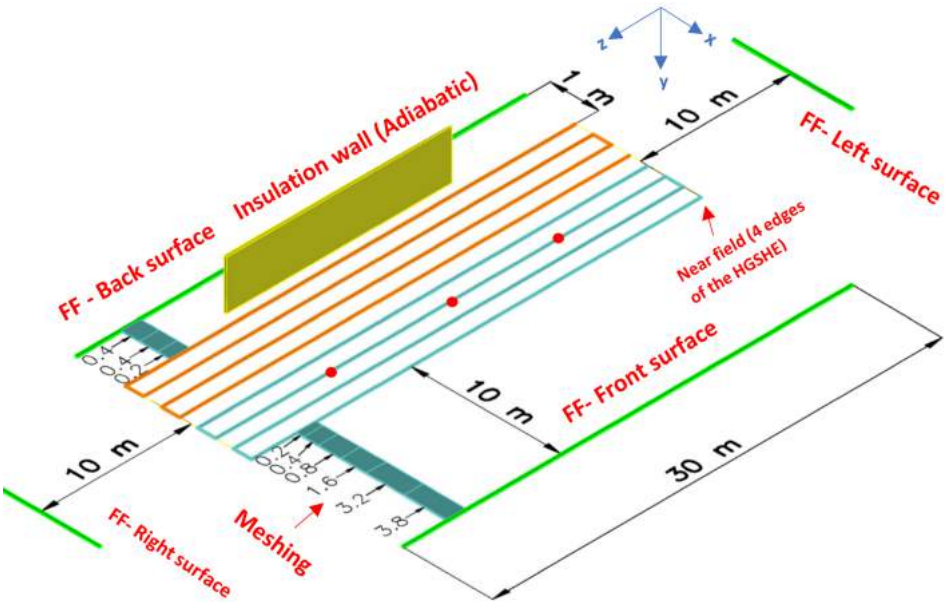

Figure 3.1: 2D boundary conditions HGSHE model.

In the model is defined the near field and the far field (FF), the first one is contained

within the 4 edges of the HGSHE and a specific depth, the other field establishes no heat transfer conduction beyond the 4 surfaces (right, left, front and back). 1 m away from one of the edges of the HGSHE, an insulation wall was installed, this barrier starts in the same level where the pipes are located (1 m below the soil surface). The length of the wall is 15 m and for the analysis, it is considered that it is located in the middle of the back surface. The back surface is considered as an adiabatic surface (not heat transfer across the surface). In the others surfaces, heat conduction is possible. The right, left and front surfaces are located 10 m away from the edges, the depth considered for the analysis is 9 m below the HGSHE.

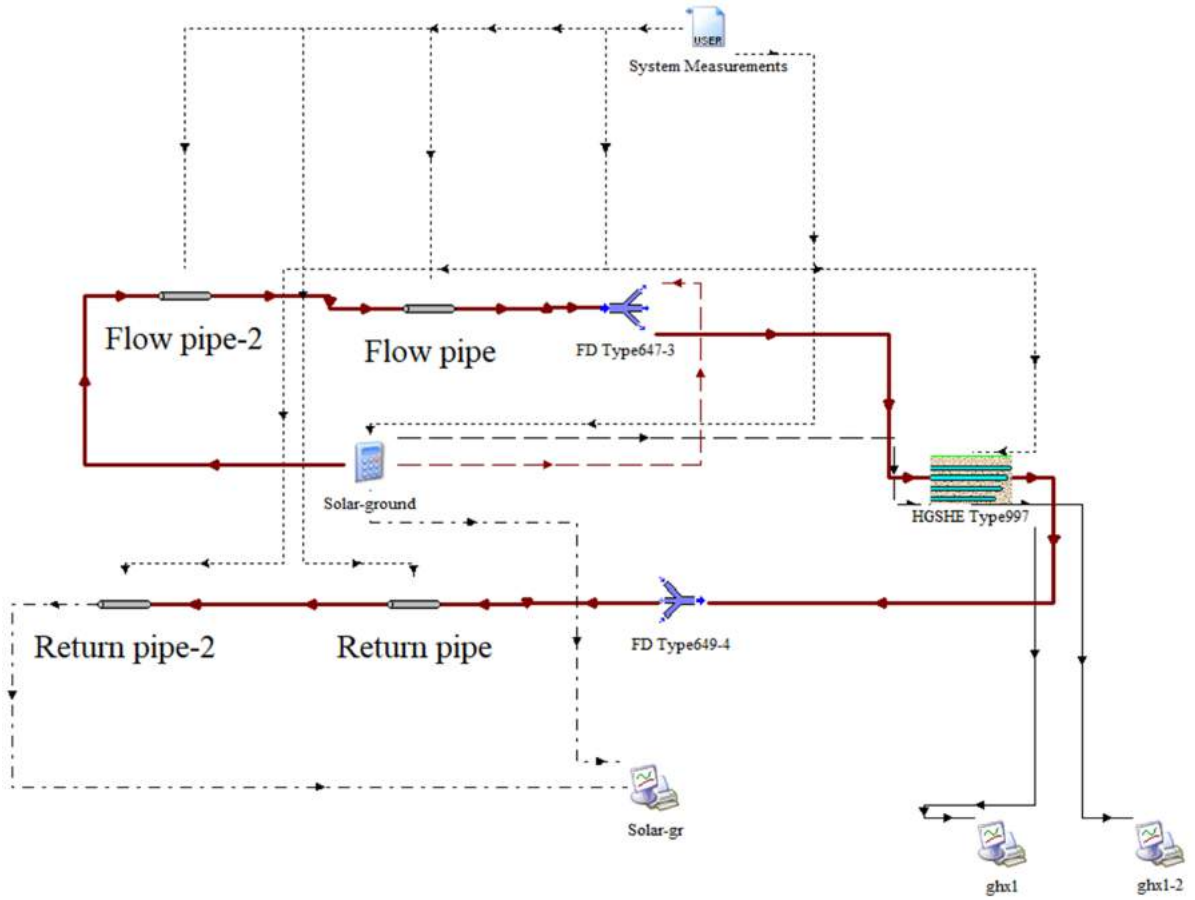

Figure 3.2: HGSHE TRNSYS model.

Figure 3.2 shows the model of the HGSHE on TRNSYS. The input data for the TRNSYS model (System measurements) is based on the measured data file (temperatures, flows, energies) and from the solar radiation data. The starting point of the model is the icon called "Solar-ground", this icon contains the inputs and the outputs to be calculated using different equations. The component "Flow pipe-2" represents the start pipe which is located inside the facility, this pipe is linked with the indoor temperature. This component is connected with the component "Flow pipe" which is the outdoor pipe and it is exposed to ambient temperature. Continuing with the circulation process, the outdoor pipe is connected to a flow diverter (FD) type 647-3. The FD represents the manifold in the prototype, in this point, the full flow is divided by 2 due to the fluid is divided into the 2 slings. The link between both elements can be seen in figure 3.3.

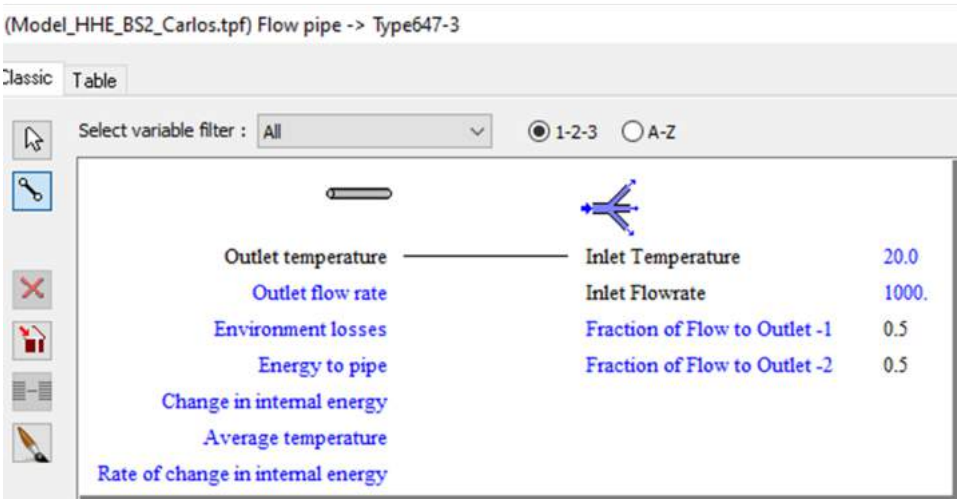

Figure 3.3: Connection between pipe and flow diverter.

The inlet temperature of the FD is the outlet temperature of the flow pipe component. Following the sequence, the outputs of the FD are the inputs for the HGSHE type 997. In terms of this component, it is set a number of pipes equal to 8, these are divided into 4 volumes in order to emulate the ground temperature sensors located close to the pipes. This means that 4 temperatures will be calculated along the pipes. Also, it must be defined the flow direction for every pipe considering the change of the direction of the flow between one pipe and the next one.

In order to complete the circulating cycle, the fluid has to return to the initial point. After the fluid circulated through the HGSHE, a FD type 649-4 is connected to the system and the flow which comes out it will be the full flow. A return pipe which is outdoor pipe and the return pipe-2 which is located inside the facility complete the components of the system. In terms of the fluid, different parameters must be set for the simulation, density (ρ), thermal conductivity (k), viscosity (μ), specific heat (Cp).

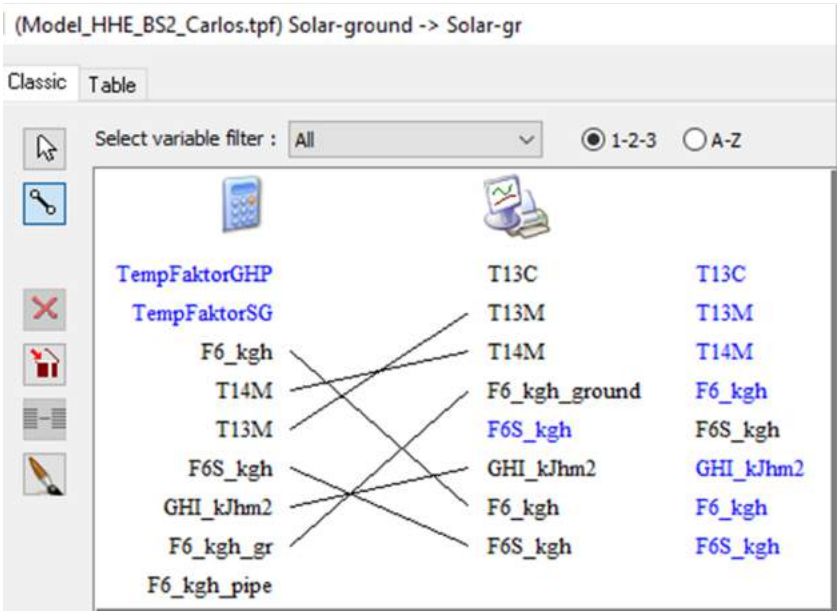

Figure 3.4: Inputs and Outputs TRNSYS model.

The pipes and the HGSHE are linked to the System measurement file (black dotted lines figure 3.1). The Solar-gr icon is linked with the return pipe-2 and the Solar-ground icon in

order to calculate the different outputs, the output file with the different results is contained in the solar-gr icon. The outputs of the simulations and how the parameters are linked are shown in the figure 3.4. 2 more output files are generated via the icons ghx1 and ghx1-2, these are not used in this analysis.

3.2 Soil model on TRNSYS

In order to establish the interaction between the soil and the HGSHE, a soil mesh must be generated. This three-dimensional mesh is based on finite elements, this means that the soil is divided in small volumes nodes. For the analysis, it is considered the smallest node size equal to 0.2 m and it is used 2 as multiplier factor. An example of the generation of the grid values can be seen in the figure 3.1 for the front and back surface. Considering the back surface, the meshing process generates 3 volumes nodes (lengths on axis x: 0.2 m, 0.4 m and 0.4 m). The last value is equal to 0.4 m instead 0.8 m (which is 2 times 0.4 m) to complete the 1 m length.

It is considered one type of soil for the analysis with constant properties (density of the soil layer, specific heat of the soil layer and thermal conductivity). In terms of the heat transfer process, it is established boundary conditions on the surfaces. The front, right and left surfaces will allow conductive heat transfer. On the other hand, the back surface is considered adiabatic.

3.3 Start temperature profiles

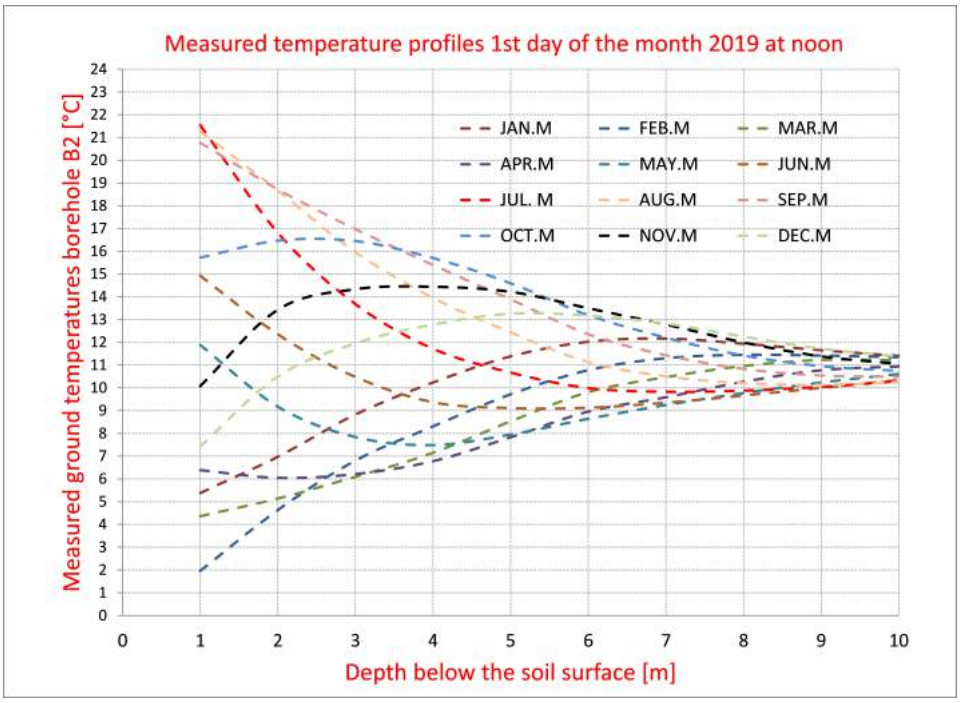

Figure 3.5: Measured temperature profiles 1st day of the month 2019 at noon .

In order to set the ground parameters on TRNSYS, it is needed to calculate and determine some of them. Specifically, the T_{ave} parameter which is the average deep earth temperature and the amplitude of T_{ave} which indicates the variation considering T_{ave} as base line. Considering the soil measured data from -1 to -10 m below the surface in the borehole B2, a profile

temperature is generated in order to establish the temperatures distribution under the soil. Due to the temperatures vary during the day, it is selected the measurement of the first day of each month at noon as reference. Figure 3.5 shows the monthly temperature.

In order to set the start temperature conditions on the ground, it is used the Kusuda correlation [8]. The boundary condition temperature T_{BC} calculates the temperatures at depth 'z' on any day of the year, This parameter will be used to generated temperature profiles at depth from -1 to -10 m at noon and compare them with the previous generated temperature profiles. The aim is to generate temperature profiles which fit as close as possible. Equation 3.1 shows the Kusuda correlation.

$$T_{BC}|_{z,day} = T_{ave} - T_{amp} * exp(-z(\frac{\pi}{365 * \alpha_{soil}})^{0.5}) * \cos(\frac{2\pi}{365}(Day - Day_{min} - \frac{z}{2}(\frac{365}{\pi * \alpha_{soil}})^{0.5})) \tag{3.1}$$

The different parameters of the equation 3.1 are inputs on the TRNSYS model. Since k, ρ and Cp are considered constant values for the analysis, the thermal diffusivity of the soil (α_{soil}) is also a constant due to this parameter is function the previous parameters. Day_{min} is the day of the year with minimum surface temperature. T_{ave} is the average deep earth temperature in the model, this temperature is set 10 m below the surface. T_{amp} is the amplitude of T_{ave}.

Figure 3.5 shows an average ground temperature 10 m below the surface around 11° C for all the months, therefore, 11° C is selected as the average deep earth temperature during the year (T_{ave}). In order to set the best T_{amp}, an iteration is carried out until the best suitable value is found. Figure 3.6 shows the calculated and measured temperature profile the 1st of July at noon. In this month the best suitable T_{amp} value is 17. Table 3.1 shows the monthly T_{amp} values.

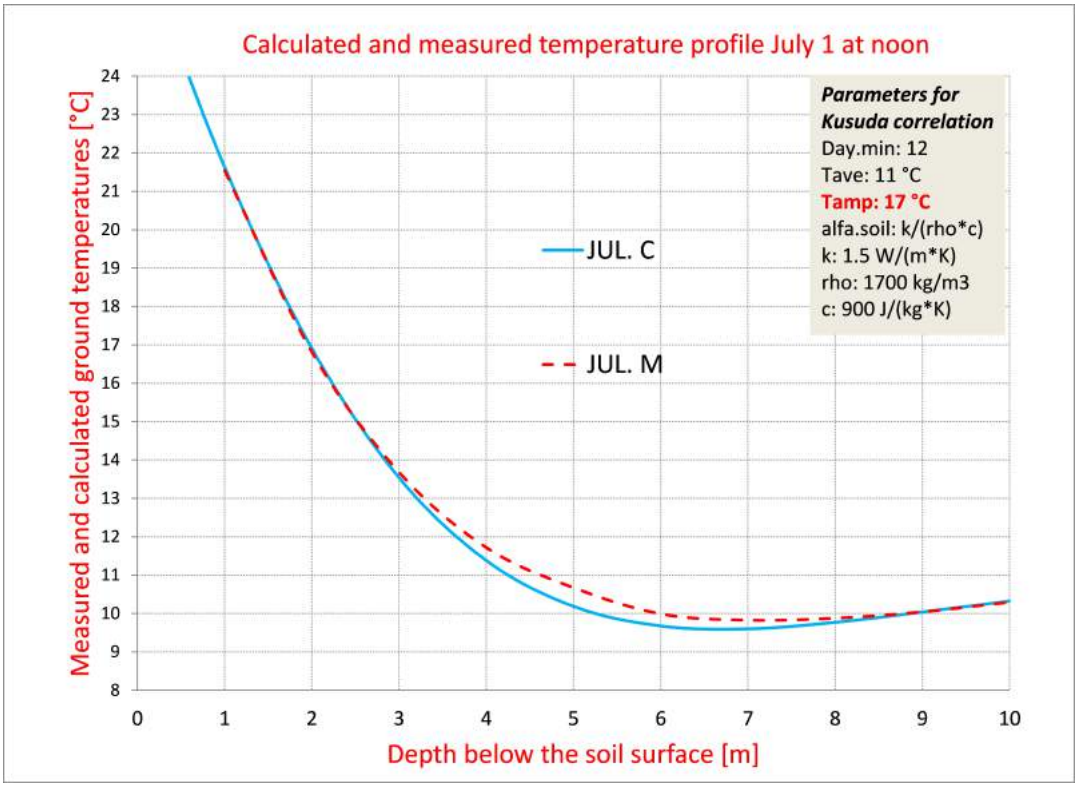

Figure 3.6: Calculated and measured temperature profile July 1 at noon.

Month	Amplitude of deep earth temperature (°C)
January	10
February	12.4
March	11
April	12.8
May	14.5
June	11.3
July	17
August	15
September	15.5
October	15
November	16
December	11.5

Table 3.1: Monthly T_{amp}.

3.4 Pipe soil contact resistant (PSCR) and Simulations

In terms of the PSCR parameter, this varies according the ambient conditions during the year. The aim is to find a suitable monthly value in order that the difference between the calculated outlet temperature (T13 C) in the simulation and the measured temperature T13 in the prototype (T13 M) be as low as possible. If the ΔT difference is lower (T13 M -T13 C), the approach is more accurate. The PSCR is a parameter which establishes the resistance to heat transfer between the soil and the pipe, lower values of PSCR indicate a higher heat transfer between the pipe and soil. Different simulations are done on TRNSYS different PSCR values in order to find a good low ΔT difference. An illustration of the simulation is shown in figure 3.7, the results of the simulations are presented below.

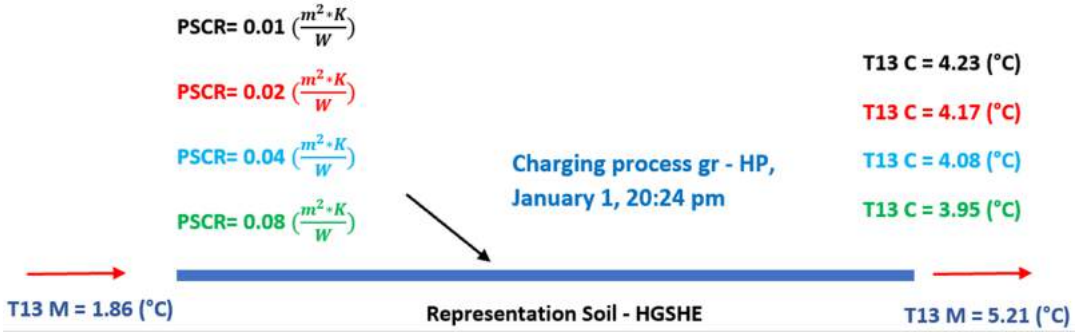

Figure 3.7: Iteration method PSCR January 1.

Figure 3.8 shows the ΔT difference with different PSCR values in terms of the inlet temperature T14 M. Values lower than -0.5°C are selected for T14 in order to have a better distribution of the values,this period correspond to January (operational mode gr- HP). Notice that when the PSCR value is lower, ΔT difference is lower, therefore, the heat transfer process is higher. For PSCR values lower than 0.01, the ΔT difference does not change significantly. Figure 3.9 shows a higher ΔT difference when the SC transfer heat to the ground, few measurements over the period can contribute to have a poor resolution of the results. For this month, a PSCR value equal to 0.01 determine suits well for both operational modes, this means that the process has

the same resistant no matter if heat is extracted from the soil or provided via the SC operation.

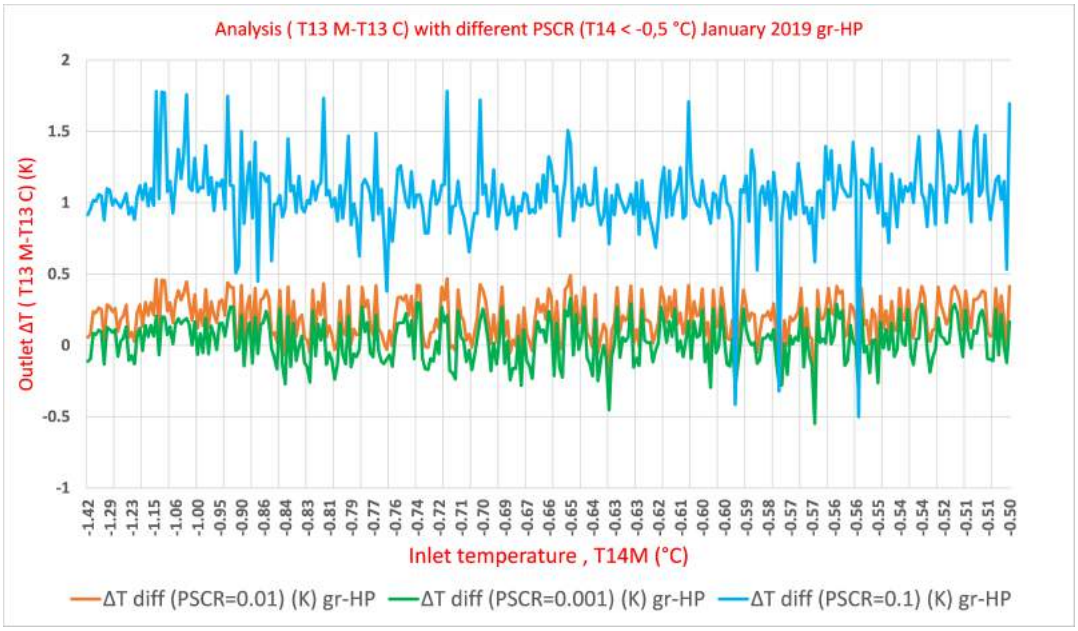

Figure 3.8: Analysis (T13 M-T13 C) with different PSCR (T14 < -0.5 °C) January 2019 gr-HP.

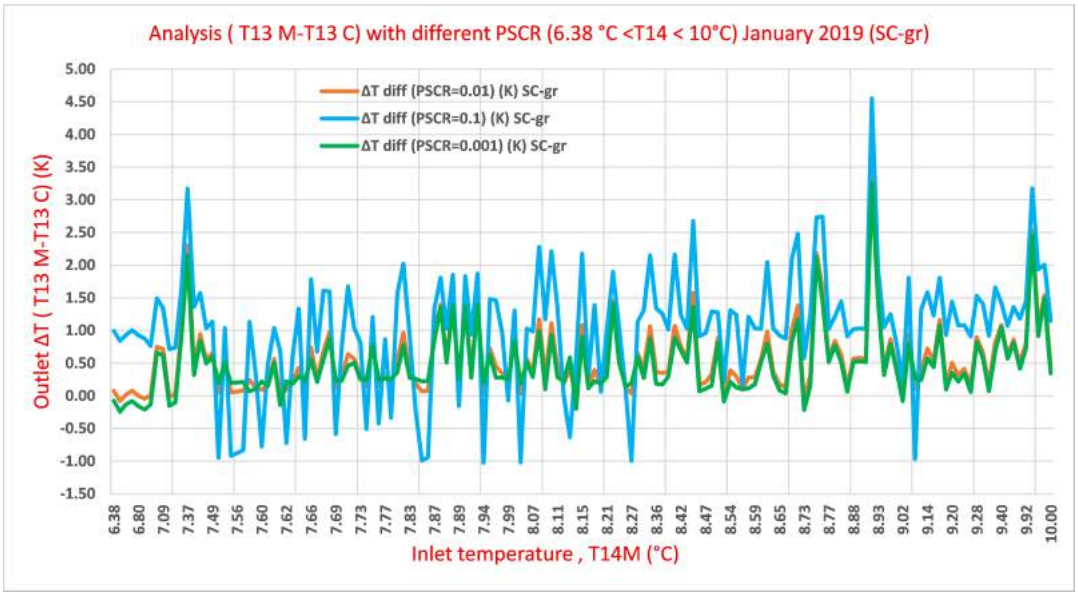

Figure 3.9: Analysis (T13 M-T13 C) with different PSCR (6.38 °C <T14 < 10°C) January 2019 (SC-gr) .

Figure 3.12 shows the ΔT difference for different PSCR values considering 4 T14 intervals on January (gr-HP mode). For all the intervals, a low PSCR results in lower ΔT differences. For intervals with higher values, the ΔT difference will be higher and the trend is the same.

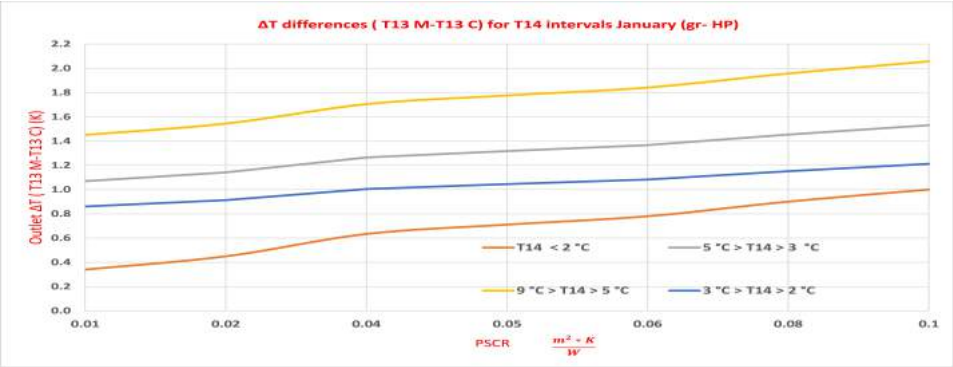

Figure 3.10: ΔT differences (T13 M-T13 C) for T14 intervals January.

Considering July, figure 3.11 shows the ΔT difference in function of T14 M for different PSCR values (SC-gr mode). In this case, the lowest ΔT difference is linked with a PSCR value equal to 0.05. It was expected than on summer the PSCR value will be higher due to the ambient conditions, in these periods, the contact between the pipe and the soil is less since the soil is dryer and the interface soil - pipe is not the optimal to transfer heat.

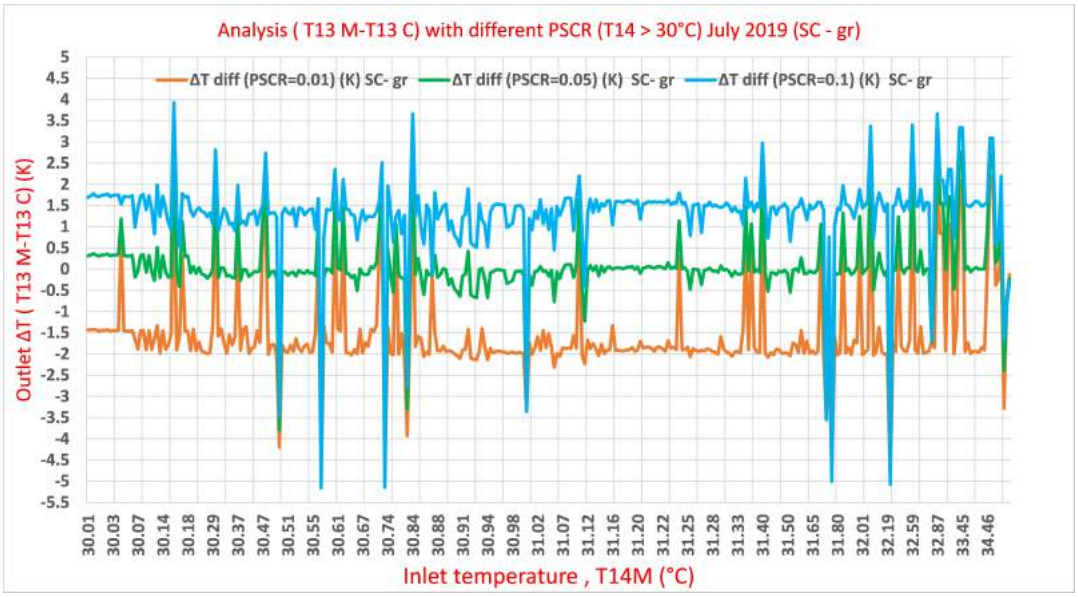

Figure 3.11: Analysis (T13 M-T13 C) with different PSCR (T14 > 30°C) July SC-gr.

Figure **??** shows the ΔT difference for different PSCR values considering 4 T14 intervals on July (SC-gr mode). It can be seen a different behavior in comparison with the same analysis on January. A decreasing tilt of the ΔT difference value for T14 M until 20°C when the PSCR is higher and lower ΔT difference values for a PSCR equal to 0.05 for temperature higher than 20°C.

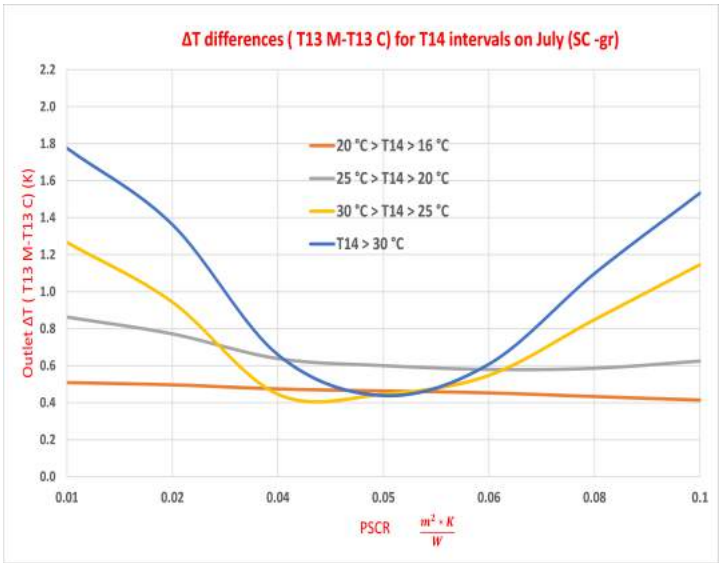

Figure 3.12: ΔT differences (T13 M-T13 C) for T14 intervals July.

Figure 3.13 shows the different PSCR values through all the years, low values on winter where the heat transfer is and low values on summer. In some months, the PSCR values is slightly different. Low number of measurements or short operational periods affect can affect. In general, longer periods generate steady state conditions and this makes possible to calculate more accurate results.

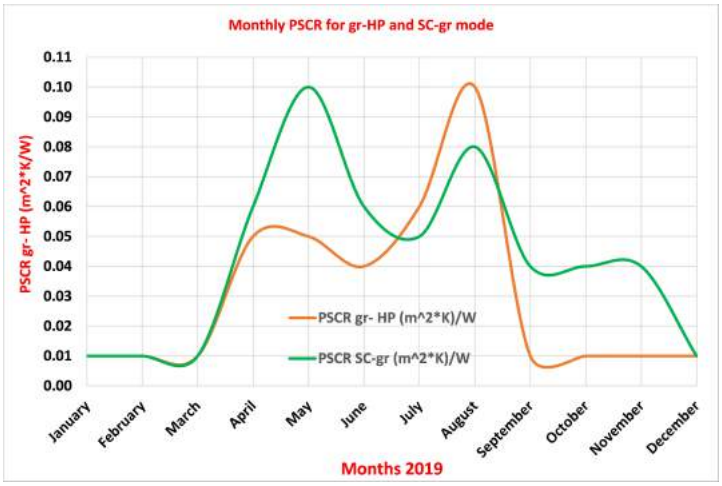

Figure 3.13: Monthly PSCR values for both operational modes.

Figure 3.14 shows the TRNSYS simulation on January, it is graphed the measured inlet temperature (T14 M), T13 M and T13 C. Also is shown the flow inside the HGSHE (pump F6) in $\frac{kg}{h}$. It is noticed that T13 C is slightly higher than T13 M during the operation of the heat pump. T13 C change is more notorious in larger periods when the heat pump is working, no present peaks as T13 M does, the range of fluctuation is quite short if we compare with the amplitude of T13 M.

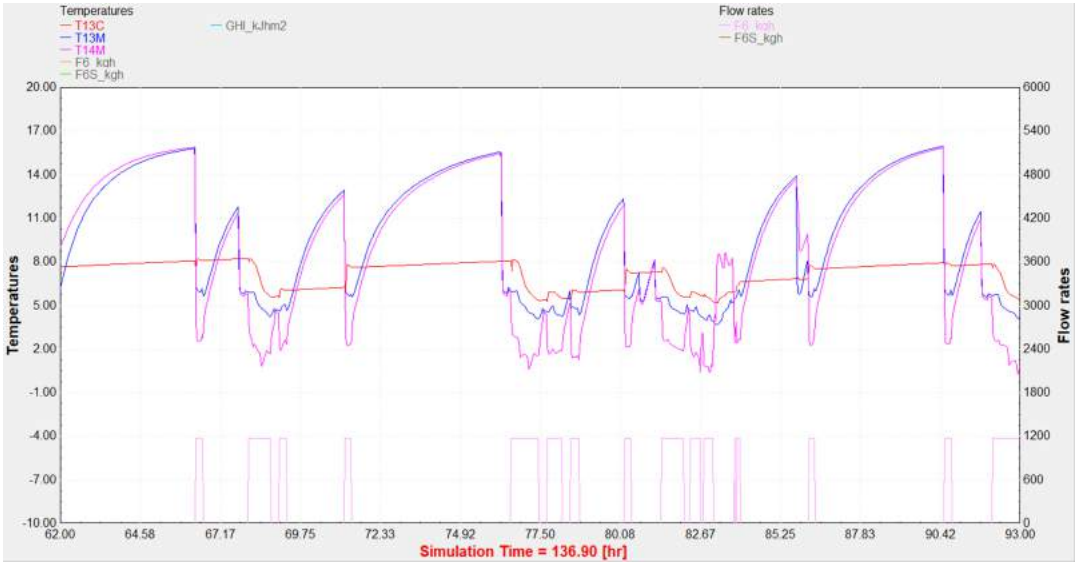

Figure 3.14: TRNSYS simulation January 3.

Figure 3.15 shows a simulation for July 23 when the SC provides heat to the soil. It can be seen the peaks on T14 M, this is related with the operational condition of the pump P3, which stops every 20 min to evaluate the conditions of the system. In these periods, T14 M increase its value since no heat is transferred to the soil. It can be seen also the time ahead of the measurements. For this period, it seems that T13 C has transferred less heat to the system in comparison with T13 M since T13 C has a higher value than T13 M.

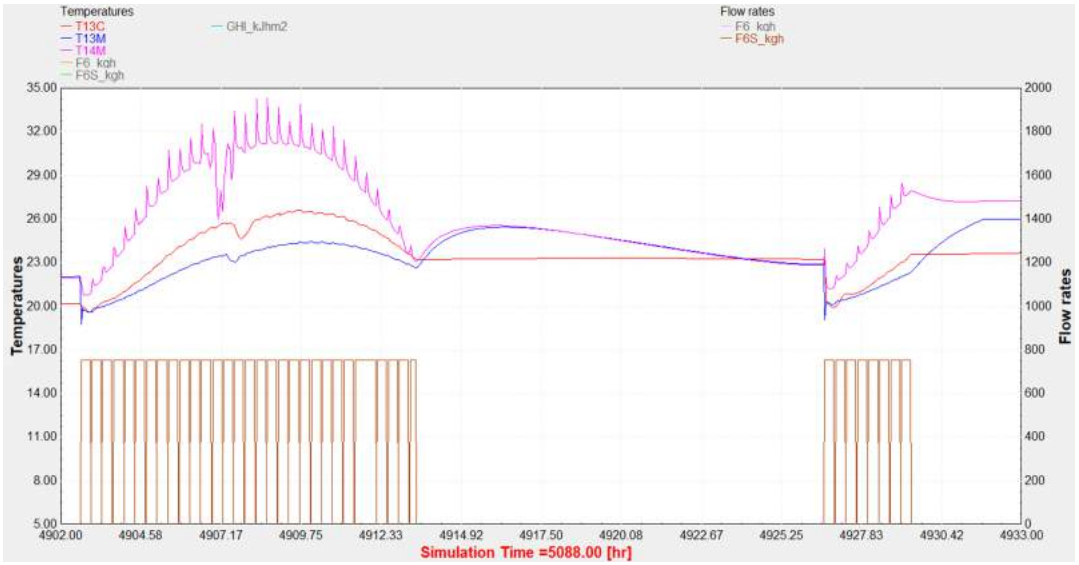

Figure 3.15: TRNSYS simulation July 23.

CHAPTER 4

Results

In this section is presented the calculation of the energy quantities in the system and the monthly seasonal performance factor (SPF). Before to explain the analyzed cases, it is necessary to establish some concepts. The energy consumed in the operation is related with the different pumps, the control systems and the motorized valves which direct the flow according the operational mode. The last 2 factors (motorized valves and control systems) will be named parasitic energy. 4 performances are analyzed:

- The SPF considering the scenario which the heat pump is in operation and its relation with the parasitic energy (Eq. 4.1) and additionally, the pump energy consumption in this operational mode (Eq. 4.2).
- The SPF similar to the Eq. 4.2, including the energy transferred to the ground and to the tank from the solar collector (Eq. 4.3) (it is included all the pumps energy consumption of the system).
- The SPF considering the energy output (SH and DHW) and the energy input (parasitic energy and pumps energy consumption) (Eq. 4.4).

$$SPF_{HP} = \frac{\sum Q_{HP}}{\sum(E_{ctsHP} + E_{mvHP})} \tag{4.1}$$

$$SPF_{(HP)tot} = \frac{\sum Q_{HP}}{\sum(E_{ctsHP} + E_{mvHP} + E_{cpHP})} \tag{4.2}$$

$$SPF_{HP+SC} = \frac{\sum (Q_{HP} + Q_{solar(gr+tank)})}{\sum(E_{cts(solar+HP)} + E_{mv(solar+HP)} + E_{cp(solar+HP)})} \tag{4.3}$$

$$SPF_{(SH+DHW)} = \frac{\sum(Q_{SH} + Q_{DHW})}{\sum(E_{cts(solar+HP)} + E_{mv(solar+HP)} + E_{cp(solar+HP)})} \tag{4.4}$$

Figure 4.1 shows energy quantities of the system in 2019, it was not considered periods with malfunction which turn out in inaccurate results. The greatest values of energy are provided by the heat pump to the tank on winter. On the other hand, the operation of the heat pump is low on summer, the energy to produce DHW and SH is provided by the solar collector in those months.

Figure 4.2 shows the seasonal performance factors for the analyzed cases, the heat losses are neglected in the analysis. Considering the first case (Eq. 4.1), the SPF value is very similar on winter (around 3). On summer, the SPF for this scenario is low due to the low contribution of energy to the system. In the case of $SPF_{(HP)tot}$, the value is similar to the SPF_{HP}, this indicates that the pump electricity consumption does not affect considerable to the performance.

In terms of SPF_{HP+SC}, this SPF has the greatest values in the analysis, the main contribution is related with the energy transferred to the ground from the solar collector from April

to August. During these months, the production of DHW and SH are satisfied, and the energy is transferred to the soil as second priority. The last performance, $SPF_{(SH+DHW)}$ presents similar values on winter, on summer the value is lower since no SH is produced.

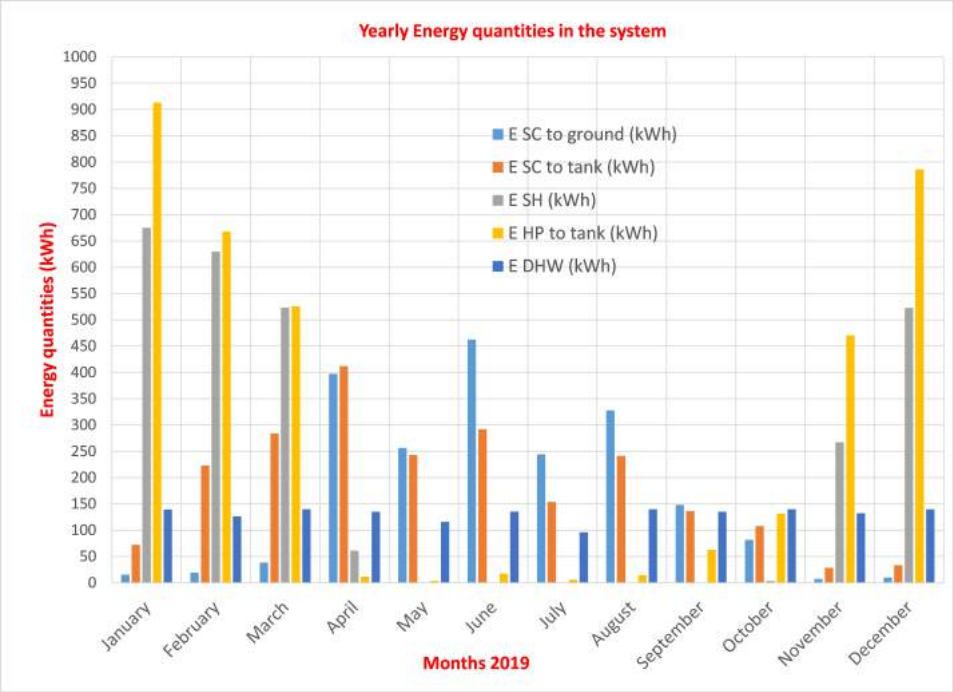

Figure 4.1: Energy quantities 2019.

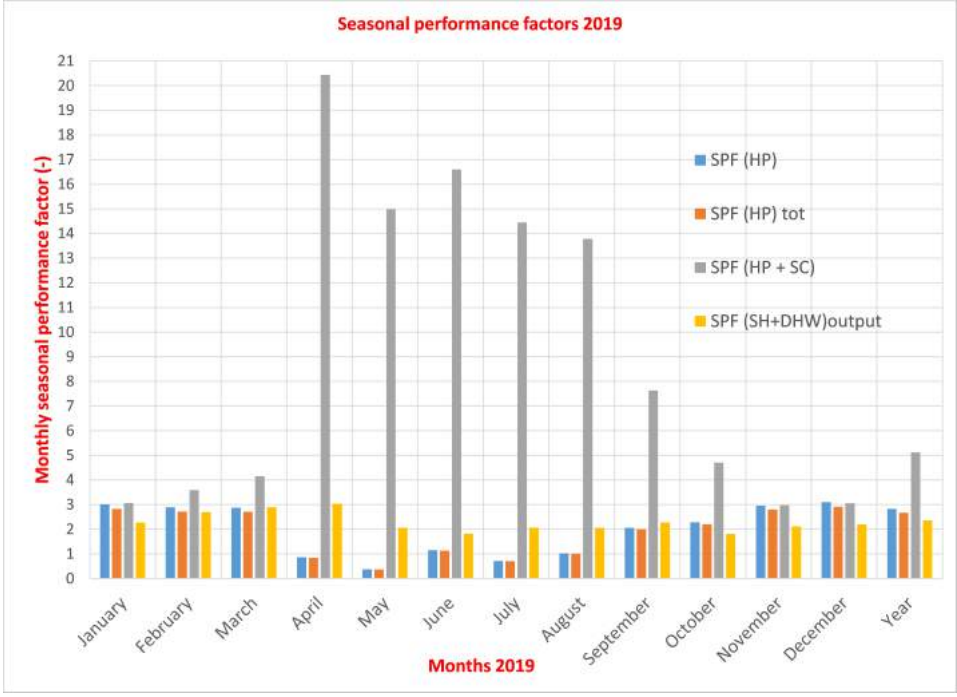

Figure 4.2: Seasonal Performance Factors (SPF).

CHAPTER 5

Conclusion

- The analysis of combined solar - heat pump systems helps to understand of a better way the heat and mass transfer in different operational modes of the system.//
- The study of this kind of systems is complex, but the potential for the application on different fields in short time is very important considering that renewable energies are involved in this prototypes.
- The analysis of the solar radiation on the ground shows that inertia of the soil tries to keep the current temperature conditions, this was shown in different graphs where the temperature under the soil was not affected by the solar radiation immediately. Changes were seen after some hours of the exposition to important values of solar radiation.
- The ground close to the pipes were affected by the system when this was in operation. It could be seen similar ground temperatures and fluid temperatures when heat was provided or extracted from the soil. The influence of the process does not extend long lengths from the edge of the HGSHE. The sensor located beside the edge of the HGHE in borehole B2 does not measure a change of the temperature when the system is on operation.
- The calculations on the same fluid volumes results in more accurate results.
- Since the resolution of the thermometers is low, it is difficult to establish a conclusion in terms of the affectation of the rain on HGSHE heat transfer.
- intermediate measures of the fluid inside the HGSHE can facilitate the analysis of the heat transfer between the pipes and the soil.//
- The calculation of the energy quantities based on the is a energy consumption of the components and flows of the pumps is a good approach to develop a numerical model of the system.
- The power generated in the system is higher when the temperature of the soil is higher, this is characteristic on summer months. Ground temperatures tends to keep its current temperature, so, the difference between the temperature inside the HGSHE and the ground is higher on summer periods.
- The pump energy consumption does not affect in high degree the seasonal performance of the system. The consideration of all the components involved in the system results in a better calculation of the different seasonal performance factors.

- The model of the HGSHE on TRNSYS is a good approach to calculate the outlet temperature of the fluid (T13 C) since the results shows that the difference between the calculated and measured temperature is less than one degree.
- Low pipe soil contact resistant values on winter show that the contact between the pipes and the soil allow to transfer the heat in a better way. On the other hand, on summer those values are higher since the interface between the soil and the pipes is not the best to tranfer heat.
- The temperature of the soil 10 meters under the surface is pretty constant during the year. It can be considered as constant temperature for next investigations.

-

APPENDIX A

An Appendix

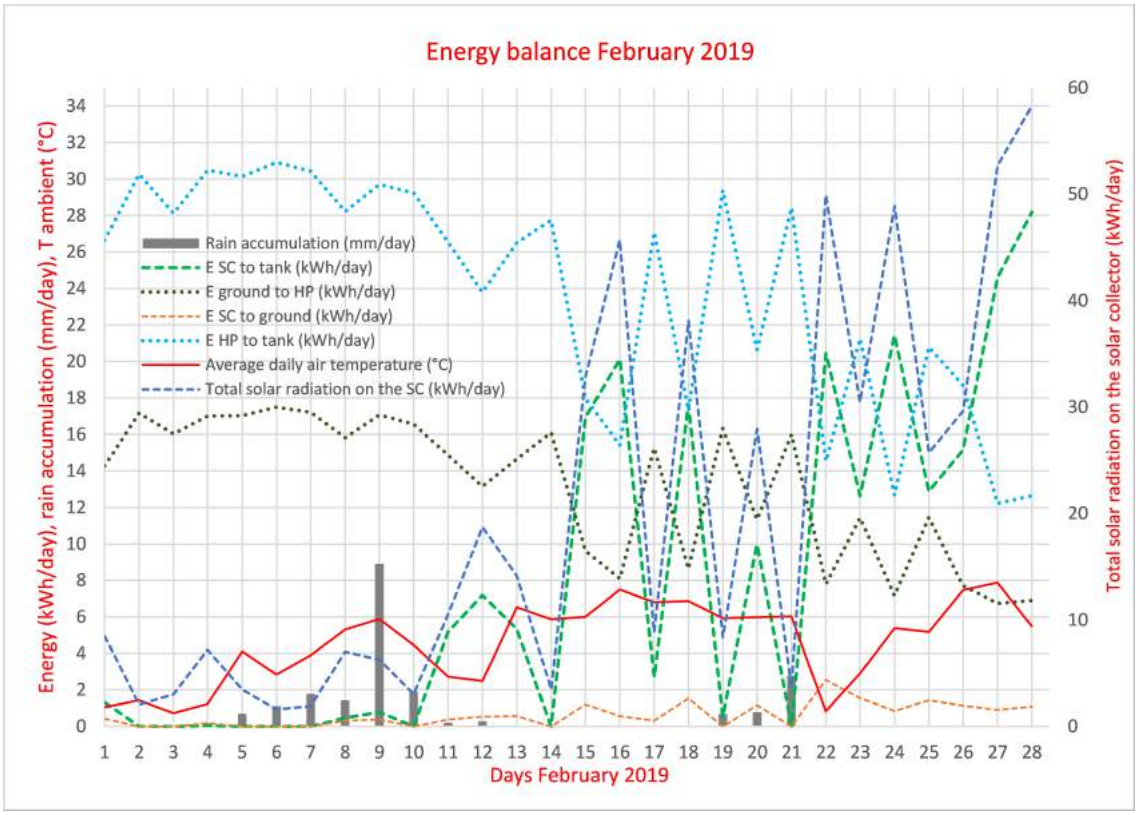

Figure A.1: Energy balance February 2019.

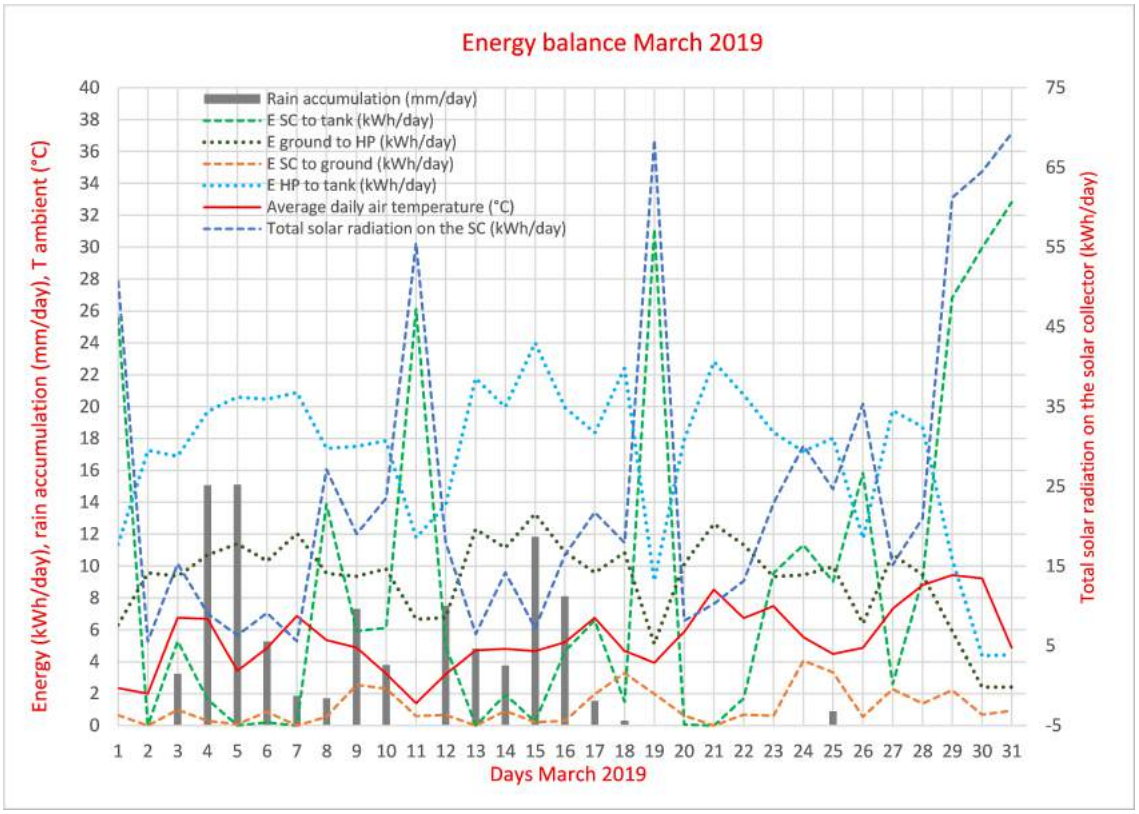

Figure A.2: Energy balance March 2019.

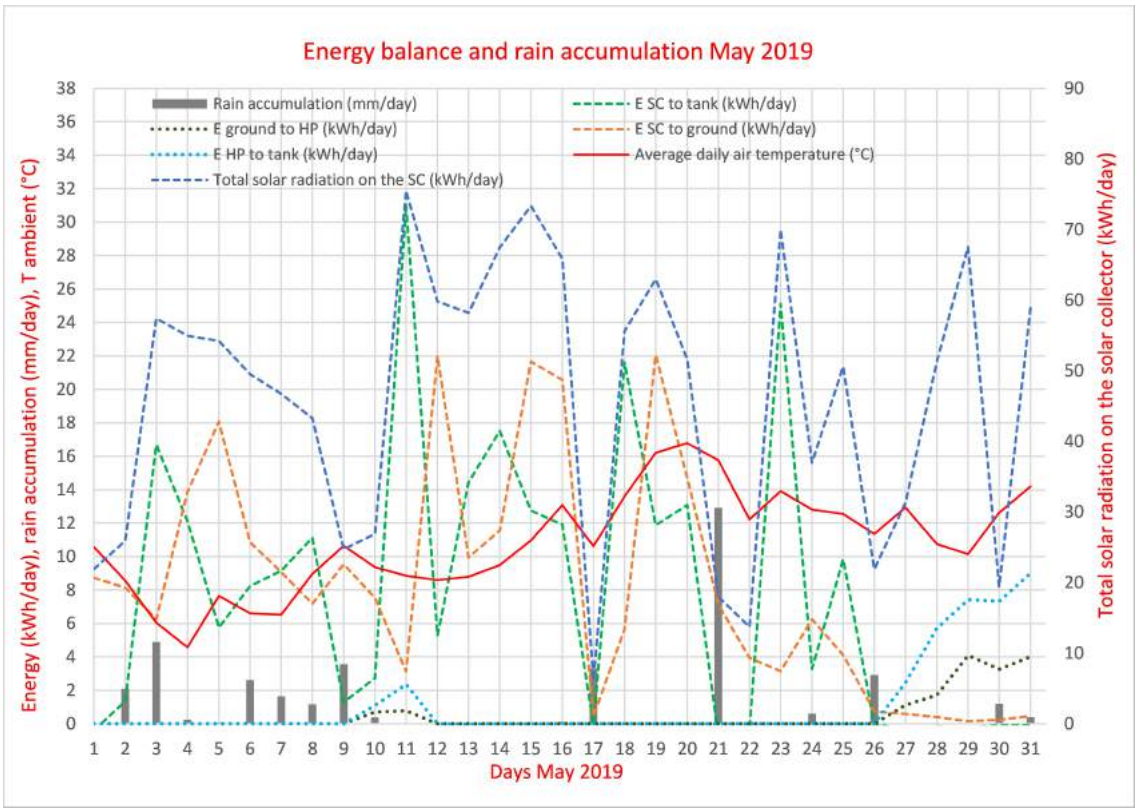

Figure A.3: Energy balance May 2019.

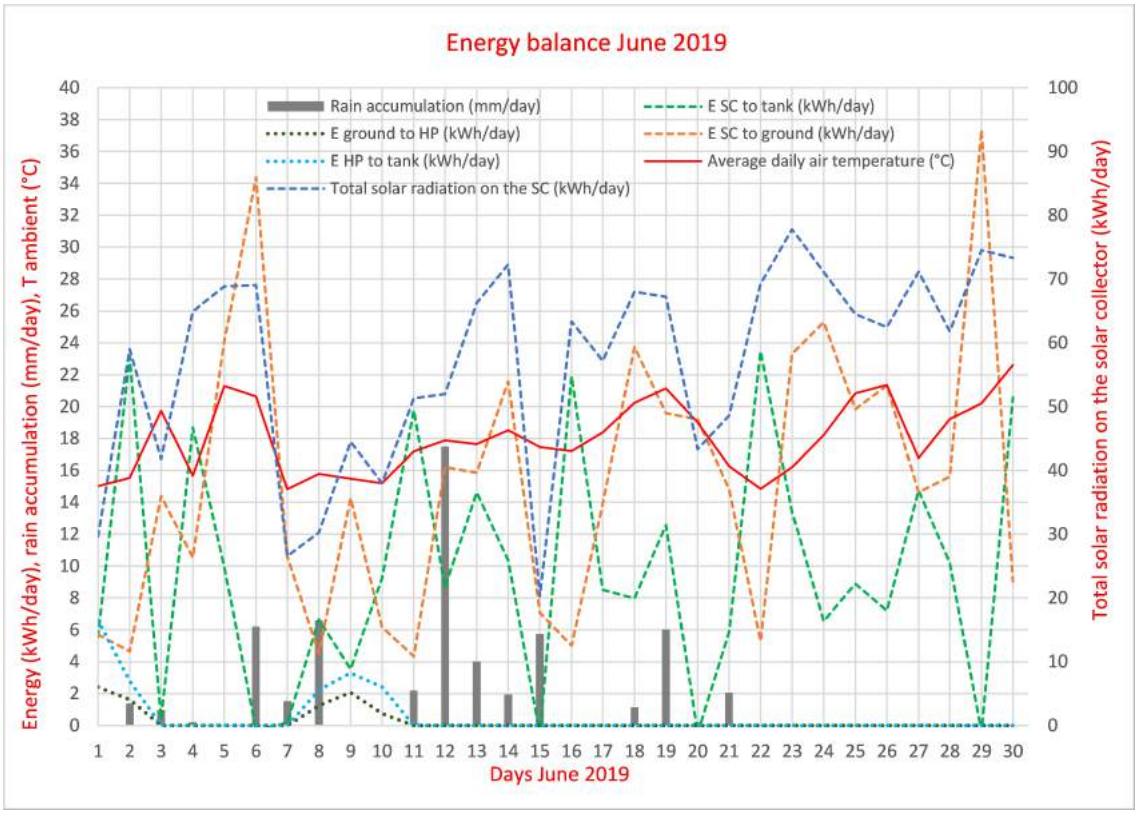

Figure A.4: Energy balance June 2019.

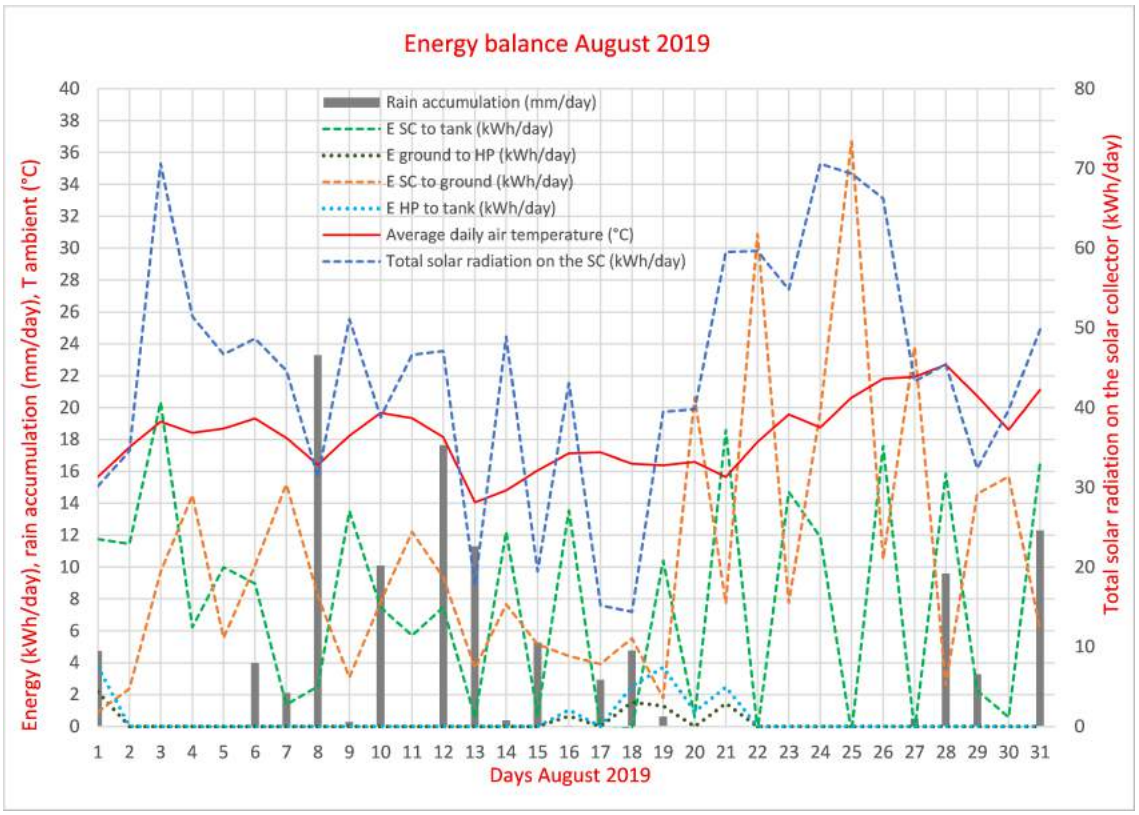

Figure A.5: Energy balance August 2019.

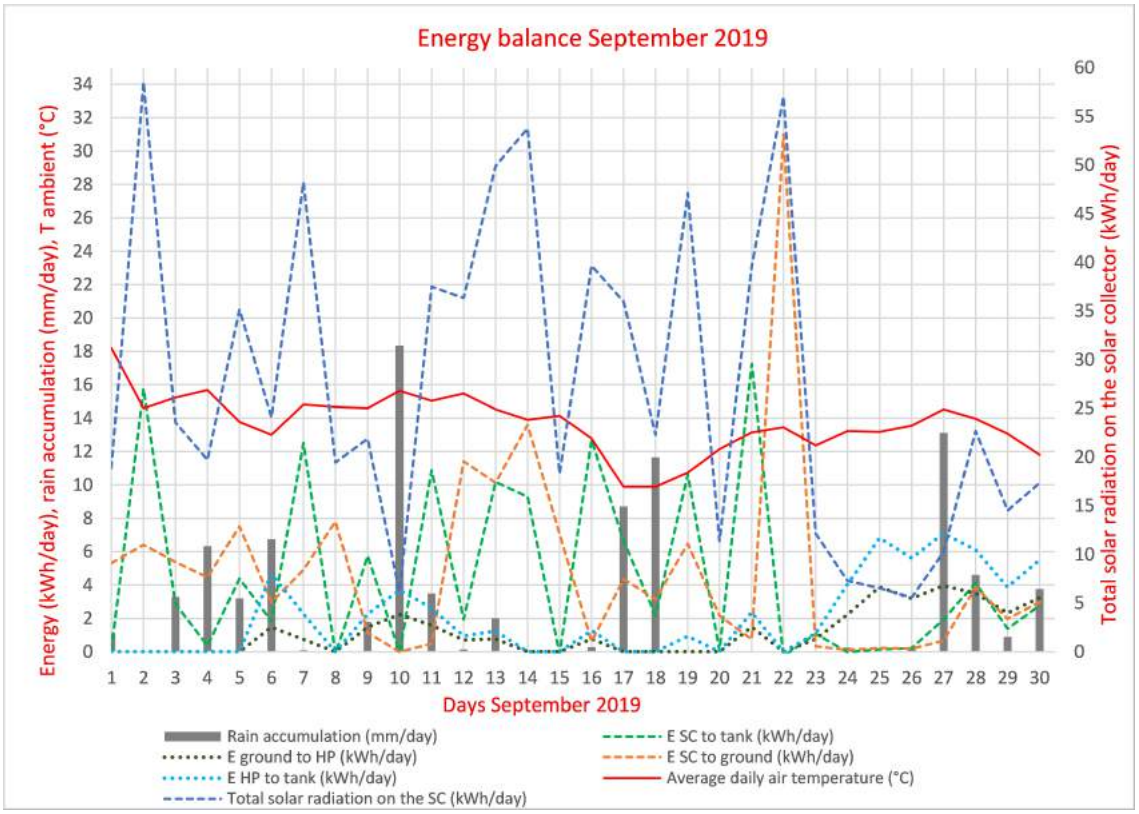

Figure A.6: Energy balance September 2019.

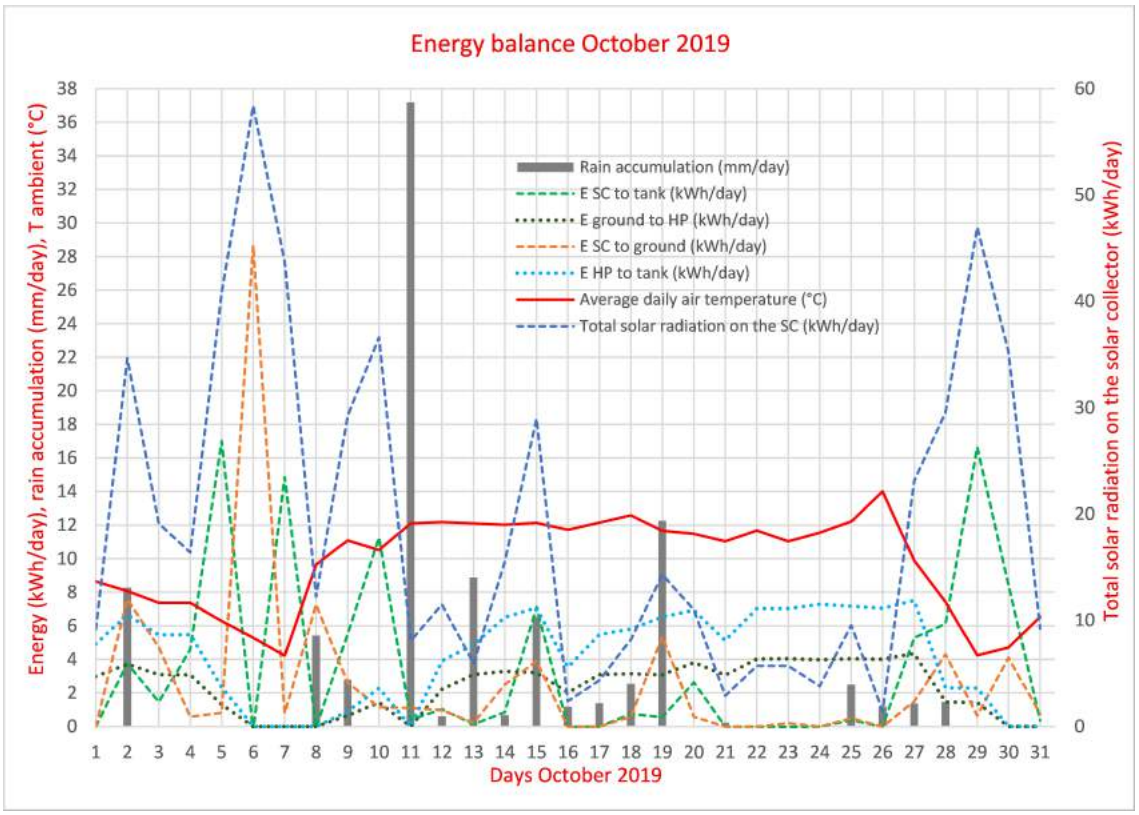

Figure A.7: Energy balance October 2019.

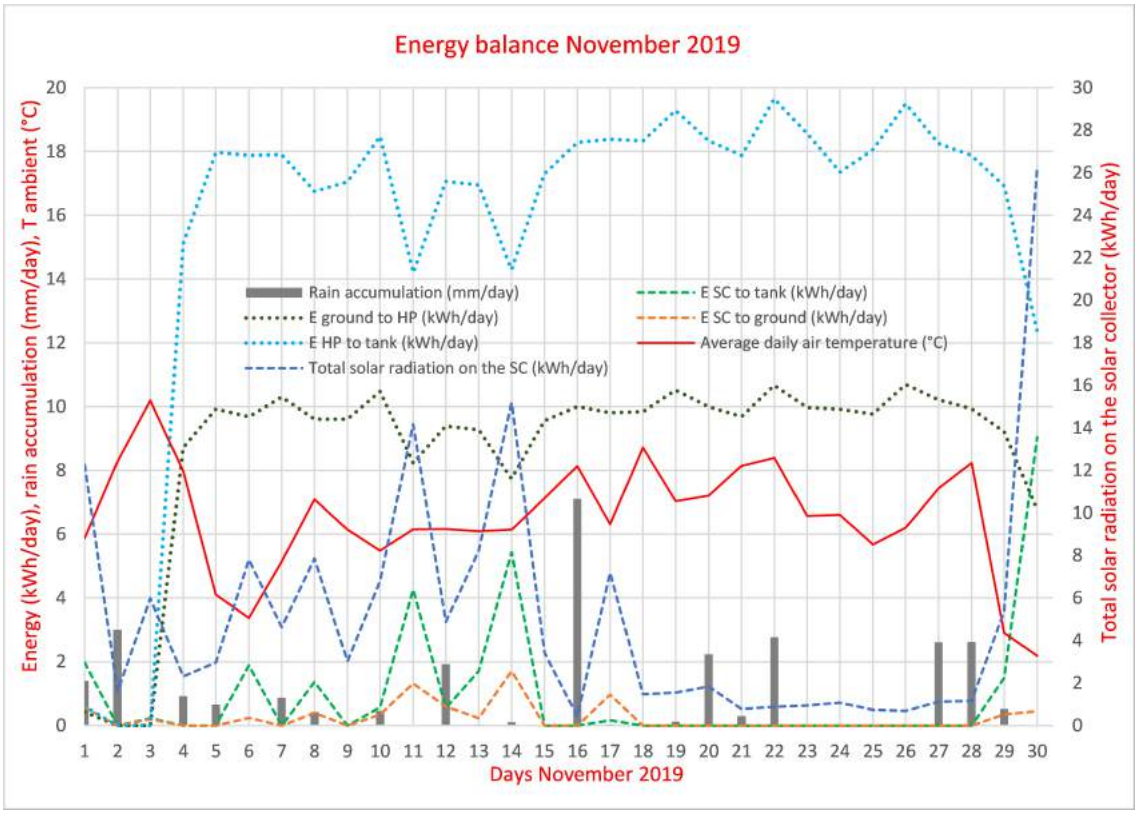

Figure A.8: Energy balance November 2019.

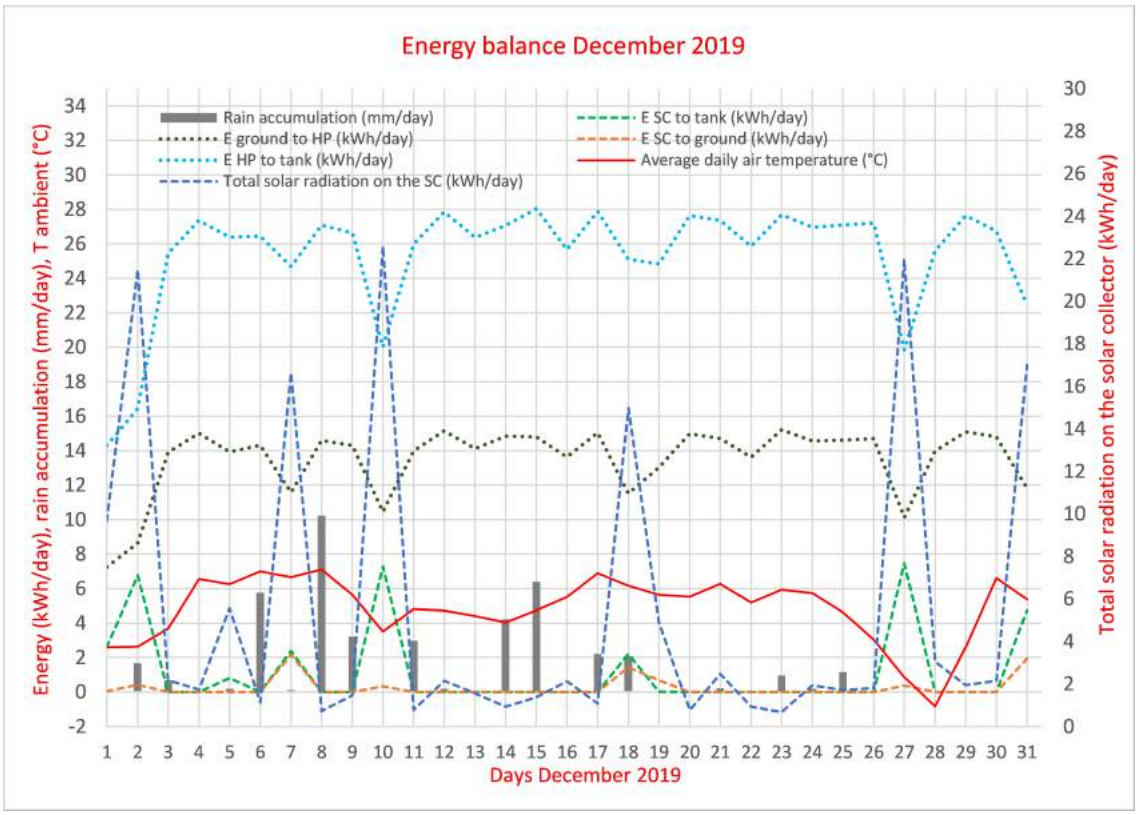

Figure A.9: Energy balance December 2019.

References

[1] J. Ann-Mari Lanty. *Solar radiation Educational note on solar radiation, 2015, Technical University of Denmark.*

[2] R. E. asameen Al-Ameen*, Anton Ianakiev. *Thermal performance of a solar assisted horizontal ground heat exchanger, 2017, Energy 140 , pag 1216-1217.*

[3] B. P. Elsa Andersen. *Experimental investigations on solar heating/heat pump systems for single family houses, 2017, Technical University of Denmark.*

[4] T. V. K. L. K. A. Elsa Andersen, Janne Dragsted. *Upgrade and Extension of the Climate station at DTU Byg, 2014, Technical University of Denmark.*

[5] H. H. Fabian Hüsing and G. Rockendorf. *COMBINATION OF SOLAR THERMAL COLLECTORS AND HORIZONTAL GROUND HEAT EXCHANGERS AS OPTIMIZED SOURCE FOR HEAT PUMPS, 2016, International Solar Energy Society.*

[6] E. F. F.J. Villalobos. *Principles of Agronomy for Sustainable ,2016, Springer International Publishing AG.*

[7] S. A. Ridha Chargui. *Determining of the optimal design of a closed loop solar dual source heat pump system coupled with a residential building application, 2017, Energy Conversion and Management 147, pag 40-54.*

[8] L. Thermal Energy System Specialists. *TESSLibs 17, Component Libraries for the TRNSYS Simulation Environment.* Volume 4, GHP Library Mathematical Reference pag 4-45. TESS – Thermal Energy Systems Specialists, 2013.